University of South-Eastern Norway

www.usn.no

FMH606 Master's Thesis 2023

Process Technology

Phase Transition in Rapid Depressurization of Liquefied Gases

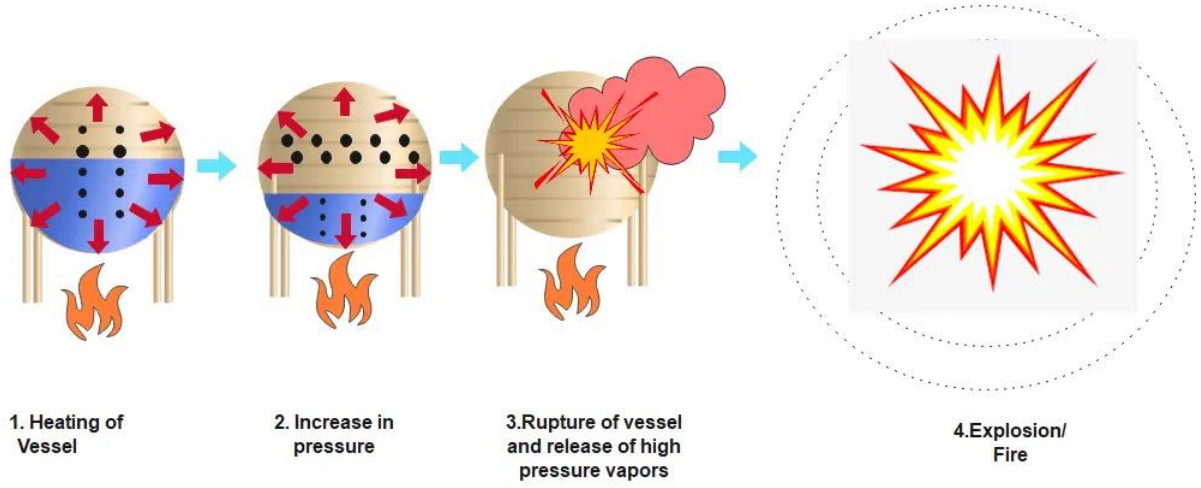

Ujjal Chandra Das

Faculty of Technology, Natural Sciences and Maritime Sciences

Campus Porsgrunn

University of South-Eastern Norway

www.usn.no

Course: FMH606 Master's Thesis, 2023

Title: Phase Transition in Rapid Depressurization of Liquefied Gases

Number of pages: 74

Keywords: Stiffened-Gas Equations of State, BLEVE, Metastable Region, Superheated Liquid, Evaporation, Phase Transitions, Depressurization, Spinodal Curve, Evaporation Waves, Thermodynamic Superheat Limit, KSL, Homogeneous Nucleation, Heterogeneous Nucleation, Evaporation Wave, Isentropic Expansion, Infinity Pressure (P∞), Ratio of Specific Heat Capacity, Evaporation Characteristics.

Student: Ujjal Chandra Das

Supervisor: Knut Vågsæther

The University of South-Eastern Norway takes no responsibility for the results and conclusions in this student report.

University of South-Eastern Norway

www.usn.no

Summary:

This thesis investigates the phase transition during rapid depressurization of liquefied gases, a crucial research field for industries like LPG storage and transportation, gas separation processes, and oil and gas production. The Stiffened-Gas equation of state describes carbon dioxide behavior during depressurization, which can lead to BLEVE (Boiling Liquid Expanding Vapor Explosions). As per the objective of this thesis, a comprehensive literature study on phase change and BLEVE has been done. To achieve the rest of goals, this study offers an in-depth exploration of carbon dioxide (CO_2) thermodynamic behavior during rapid depressurization, leveraging the Stiffened Gas Equation of State (SG-EOS) as a fundamental tool. The central objective is to attain a comprehensive understanding of CO_2's intricate thermodynamic responses in such scenarios, particularly focusing on the isentropic expansion process. This thesis discusses the selection of an EOS (Equation of State) for a BLEVE model, which is essential for describing the relationship between state variables in thermodynamic equilibrium states. The Stiffened Gas Equation of State (SG-EOS) is used to describe the metastable phase of liquids and gases under high pressure and temperature conditions. The thesis considers the properties of the SG-EOS, such as pressure, entropy, speed of sound, ratio of specific heats, Helmholtz free energy, specific enthalpy, and specific internal energy. The state calculation is done by allowing the Pressurized Liquefied CO_2 (PLG) to expand isentropically from its saturation state (293K). The thermodynamics state variables are recorded using Matlab code Thermodynamics masters from the Github Thermodynamics tool for H_2O, H_2, and CO_2. The state change data is used to evaluate SG-EOS and find suitable values for γ and $p\infty$. The density estimation is done separately for a specific set of temperatures and pressure. The investigation encompasses vital parameters, including pressure, temperature, density, and specific internal energy. The core findings and discussions revolve around the intriguing relationship between the ratio of specific heat (γ) and the infinity pressure (P_∞). The study reveals a distinctive non-linear connection between these two factors, characterized by a convex curve. The P_∞ vs γ curve has fitted best for isentropic expansion process from saturation state (293K) to 4.0Mpa. This relationship significantly influences CO_2's behavior during depressurization, especially with regards to phase transitions and explosive tendencies.

Keywords Depressurization, isentropic expansion process, Stiffened-Gas equation of state, P_∞ vs γ curve, BLEVE

The University of South-Eastern Norway takes no responsibility for the results and conclusions in this student report.

Preface

The completion of this thesis work satisfies a requirement for the University of South-Eastern Norway's master's program in Process Technology. This study aims to get in-depth knowledge about Phase Transition in Rapid Depressurization of Liquefied CO_2 gas and find out suitable values to fit in the Stiffened-Gas Equation of State in Isentropic Expansion process.

I wish to thank my supervisor, Knut Vågsæther, for his continuous support, direction, and leadership throughout the creation of my thesis. He helped me whenever I needed it, and I was able to finish my thesis successfully. He will always remain in my memory.

Finally, I would like to thank my family and friends for their stable support and inspiration throughout this difficult time but successful path.

I believe reading this thesis will provide valuable insights and contribute to the existing knowledge in the process of Phase Transition of pressurized Liquid Gas and BLEVE.

Porsgrunn, 28/05/2023
Ujjal Chandra Das

Contents

List of Figures

List of Tables

Nomenclature

Abbreviations

BLEVE	Boiling Liquid Expanding Vapor Explosions
CCS	Carbon Capture and Storage Technology
CFD	Computational Fluid Dynamics
EOS	Equation of State
KSL	Kinetic Superheat Limit
LOC	Loss of Confinement
PLG	Pressurized Liquefied Gas
SG	Stiffened Gas
SLT	Superheat Limit Temperature
TSL	Thermodynamic Superheat Limit
CO_2	Carbon dioxide

Symbols

Symbol	Name	Unit
C	Speed of sound	m/s
C_p	Specific Heat Capacity at Constant Pressure	$J{\cdot}K^{-1}{\cdot}kg^{-1}$
C_v	Specific Heat Capacity at Constant Pressure	$J{\cdot}K^{-1}{\cdot}kg^{-1}$
e	Specific Internal Energy	J/Kg
e^*	Zero point for Specific Internal Energy	J/Kg
f	Helmholtz Free Energy	J
h	Specific Enthalpy	J/Kg
P	Pressure	Pascal (Pa)

$P\infty$	Pressure infinite: SG-EOS Constant	Pascal (Pa)
S	Entropy	J/K
T	Temperature	K
T_C	Critical Temperature	K
T_{TSL}	Temperature of Thermodynamic Superheat Limit	K
γ	Ratio of Specific Heat Capacity	Unit Less
ρ	Density	Kg/m^3

1 Introduction

In the present world, due to the energy need, industrial purpose, and Carbon Capture and Storage (CCS) technology, it is very common and important to store or transport different types of liquefied gas at saturation pressures above atmospheric pressures. Investigating phase transition during the rapid depressurization of liquid gases is a crucial research field with considerable consequences for many industries. It is essential for making industrial processes more efficient and safer. Experimental and theoretical investigations are required to investigate the gas's behavior under various conditions and to create models to anticipate its behavior in different industrial procedures. Phase transitions in liquefied gases during depressurization are an essential area of research due to their relevance in various fields, such as cryogenics, gas separation processes, liquefied gas storage and transfer, and oil and gas production. The literature on this topic covers various aspects, including experimental and theoretical investigations of the phase behavior, thermodynamics, and kinetics of liquefied gases under depressurization conditions.

The Stiffened-Gas equation of state is used in this thesis' calculations to describe how carbon dioxide behaves during rapid depressurization, which encourages a phase transition and liquid carbon dioxide has been expanded isentropically. The study is limited to CO_2 behavior because of how crucial it is to CCS systems. The author believes that the same concepts also apply to other pressure-liquefied ones, though. such as ethane and propane.

The rapid phase transition of pressurized liquified gas due to depressurization can act like an explosion which could lead to blast waves that are usually called BLEVE (Boiling Liquid Expanding Vapor Explosions). Knowledge-based risk assessments are required before building the essential infrastructure to ensure the safe operation of the process facilities. A pipeline, storage tank, or vessel ruptured while holding a pressurized liquefied gas at a certain temperature boiling point exceeding atmospheric pressure is dangerous. It should be included in industrial safety assessments. Under specific circumstances, an explosion can be referred to as a boiling liquid expanding vapor explosion (BLEVE) if the rupture and subsequent release happen almost instantly. The rapid phase transition of pressurized liquified gas by sudden rupture and depressurization of the containment vessel is a violent physical

phenomenon relevant to occupational safety assessments. Under certain conditions, this phenomenon can be called BLEVE. In 1957, the term boiling liquid expanding vapor explosion (BLEVE) was coined which was done by J.B. Smith, W.S. Marsh, and W.A. Walls who were at that time with Factory Mutual Engineering Division (later renamed Factory Mutual Research Corporation and now known as FM Global)[1]. There are several definitions for BLEVE, the following are used in this thesis. "A BLEVE is the explosive release of expanding vapor and boiling liquid when a container holding a pressure liquefied gas fails catastrophically"[2]. A boiling liquid expanding vapor explosion (BLEVE) is an explosion caused by the rupture of a vessel containing a pressurized liquid that has reached a temperature above its boiling point[3], [4]. Due to sudden pressure failure in a vessel that contains pressurized liquid gas BLEVE may occur. the blast energy of a bursting vessel that contains a pressurized liquefied gas is higher than the energy estimated from a vapor-space calculation[5].

The Centre for Chemical Process Safety defines a BLEVE [6] as "a sudden release of a large mass of pressurized superheated liquid to the atmosphere".

Three key elements cause a BLEVE[6]:

1. A substance in liquid form at a temperature above its normal atmospheric pressure boiling point.
2. A containment vessel maintains the pressure that keeps the substance in liquid form.
3. A sudden loss of containment that rapidly drops the pressure.

Although often associated with fireballs or dispersion of poisonous fumes, BLEVES are also relevant for non-flammable substances such as CO_2. Hazards associated with these CO_2 releases relate to both the harmful properties of the fluid (asphyxiation and frost injuries) and the energy release (blast waves, accelerated fragments, and dynamic loads on structures).

1.1 Industrial BLEVE Accidents

Numerous incidents in the transportation and process industries can be categorized as BLEVEs. The PEMEX LPG facility in Mexico City saw arguably the worst industrial BLEVE disaster ever in 1984. The number of causalities was 650, and 6400 people suffered

injuries when 3000 tons of propane were released and ignited in a succession of BLEVEs [7]. However, a BLEVE can occur with a non-flammable substance like water or liquid carbon dioxide. The sub-sections below show examples of explosions in tanks that contained pressurized liquefied CO_2.

1.1.1 A small CO_2 BLEVE Occurred in Norway in 2008 [8]

A fire extinguisher containing 5 kg of liquid CO_2 was thrown into a waste skip bin (dumpster). Unfortunately, the skip was sent to a waste-to-energy plant where the waste was shredded before being burned. The shredder punctured the fire extinguisher and the aluminum cylinder burst into several fragments. One of the fragments, weighing 1.9 kg, flew through a two-layer steel roof and landed 35 m from the shredder.

1.1.2 Repcelok - Hungary, 1969 [7]

In the Hungarian city Repcelok, two CO_2 tanks exploded during filling in 1969. Overfilling because of a level indicator failure was the probable cause of the accident that killed nine persons. The tank pressure before the explosion was 15 bar and the temperature was -30C. The investigations concluded that the material used to manufacture these tanks was not suited for use under low-temperature conditions.

1.1.3 Worms - Germany, 1988 [9]

A 30-ton CO_2 tank exploded in the German city of Worms in 1988. The event happened at a Procter and Gamble-owned citrus processing facility in the United States. Eight people received frostbite injuries after being exposed to the CO_2's chilly air, while three people perished in the explosion. Only 20% of the tank was salvaged immediately after the explosion, and the blast waves completely devastated the neighboring structures. The remainder was discharged 300 meters into the neighboring Rhein River. A temperature of 253 K and a pressure of 2.0 MPa were used for CO_2 storage. A heater was installed in the tank to prevent freezing. Following an inquiry, it was determined that a brittle failure due to a previous low temperature (213 K) brought on by a heating system malfunction was the accident's most likely cause. The heater was restarted, but the temperature-high alert did not function. Due to overheating, the pressure in the tank was too high, and the pressure relief valve froze.

According to the studies, the tank failed at a pressure of between 3.5 and 5.1 MPa. From a CO_2 supplier, who also modified the tank soon before installation, Procter & Gamble rented the tank. This incident proved that making changes and interim fixes could raise the risk of an accident. The installation of heaters within CO_2 storage tanks was also shown to provide significant risks.

1.1.4 Yuhang, 2008; China [10]

A CO_2 storage tank exploded in Yuhang, China in 2008 when a ship was parked there. At the beginning circumstances of 2.3 MPa and 258 K, the ship was transporting 130 m^3 of liquid CO_2. Two workers at the plant were killed in the explosion, which also destroyed two neighboring ships carrying sulfuric acid and hydrogen peroxide. The level indicator and relief valve were both locked into place on the tank before the tragedy. Brittle fractures and an overfilled modified CO_2 tank were the accident's main causes.

1.2 Aims and Objectives

The main objectives of this study are given below.

1. Literature review on phase transition in liquefied gases during depressurization.
2. Continue working on model development for waves in compressible liquid and phase transition rates.
3. Develop values needed for linear equations of state.

1.3 Brief Outline of This Thesis

This thesis study is divided into five chapters. The first chapter describes the study's background and objectives. Chapter 2 describes the literature review on phase transition in liquefied gases during depressurization. Chapter 3 illustrates the methodology of this thesis. Chapter 4 includes the results and discussion. The conclusion and future research activities are discussed in Chapter 5.

2 Literature Study on Phase Transition of Pressurized Liquefied Gases

This chapter represents the understanding of phase transition in the rapid depressurization of liquefied gases. It also gives a comprehensive understanding of the thermodynamic properties of the gas, as well as the kinetics of the phase transition process. The phase transition in the rapid depressurization of liquified gases is an important phenomenon that occurs when a pressurized liquified gas is rapidly released into a lower-pressure environment. This chapter starts with the primary text about phase transition followed by superheated liquids, rapid evaporation, and BLEVE, which are relevant to the study. In the case of explosion situations, the capacity of a superheated liquid to temperately store internal energy in a metastable liquid state and then swiftly release it through an evaporation process is crucial. These phase changes occur under non-equilibrium circumstances and are distinct from "normal" nucleate boiling in thermodynamic equilibrium. The rapid evaporation of droplets near the superheat limit is then covered in this chapter. A sub-section will discuss the evaporation waves and boiling front propagation. The metastable liquid properties are also briefly studied here. An extensive review of experimental and numerical research and simulation results aimed at predicting the beginning and progression of a BLEVE is provided as the next step. A thorough analysis of the thermodynamic Equations of State (EOS) utilized in this work and a few other articles conclude the chapter.

2.1 Phase Transition in the Rapid Depressurization of Liquefied Gases

The phase transition in the rapid depressurization of liquified gases is an important phenomenon that occurs when a pressurized liquified gas is rapidly released into a lower-pressure environment. This can happen in various industrial processes, such as gas separation, petroleum production, and cryogenics. During a rapid depressurization, the sudden pressure drop can cause the liquefied gas to transition from a liquid state to a gaseous state, which can cause significant changes in the physical properties of the gas. This chapter starts with the primary text about phase transition followed by superheated liquids, rapid evaporation, and

BLEVE, which are relevant to the study. In the case of explosion situations, the capacity of a superheated liquid to temperately store internal energy in a metastable liquid state and then swiftly release it through an evaporation process is crucial. These phase changes occur under non-equilibrium circumstances and are distinct from "normal" nucleate boiling in thermodynamic equilibrium. The rapid evaporation of droplets near the superheat limit is then covered in this chapter. A sub-section will discuss the evaporation waves and boiling front propagation. The metastable liquid properties are also briefly studied here. The next step is a comprehensive overview of experimental and numerical research designed to forecast the onset and course of a BLEVE. The chapter finishes with a detailed review of the thermodynamic Equations of State (EOS) used in this study and a few other papers.

2.2 Phase Transition

Phases are states of matter with unique macroscopic characteristics. The typical phases we'll discuss in this chapter are liquid and gas. Other critical phases are compressed and metastable liquid. The appropriate variables for the phase transition are the pressure P and the temperature T. Phase transition is the process by which a material transforms from one state—solid, liquid, or gas—to another. Any element and material may transition from one phase to another at a particular temperature and pressure. Each substance has three phases. It can change into a solid, liquid, or gas [11]. The phase of materials depends on certain temperatures and pressure. The temperature and pressure at which the substance will change are very dependent on the intermolecular forces that are acting on the molecules and atoms of the substance [12]. The material also can exist in two phases simultaneously, which could be called a metastable state. In this study, the liquid and vapor will coexist at the time of transition from high-pressure liquid to gas. There are six ways a substance can change between these three phases: melting, freezing, evaporating, condensing, sublimination, and deposition [12]. Each of these processes is reversible and transitions between phases in a distinct way. This thesis study will focus on the evaporating process only. Phase transitions occur when a system's thermodynamic free energy is nonanalytic for a particular set of thermodynamic variables. This state often results from the interactions of many particles in a system and does not manifest in too-tiny systems.

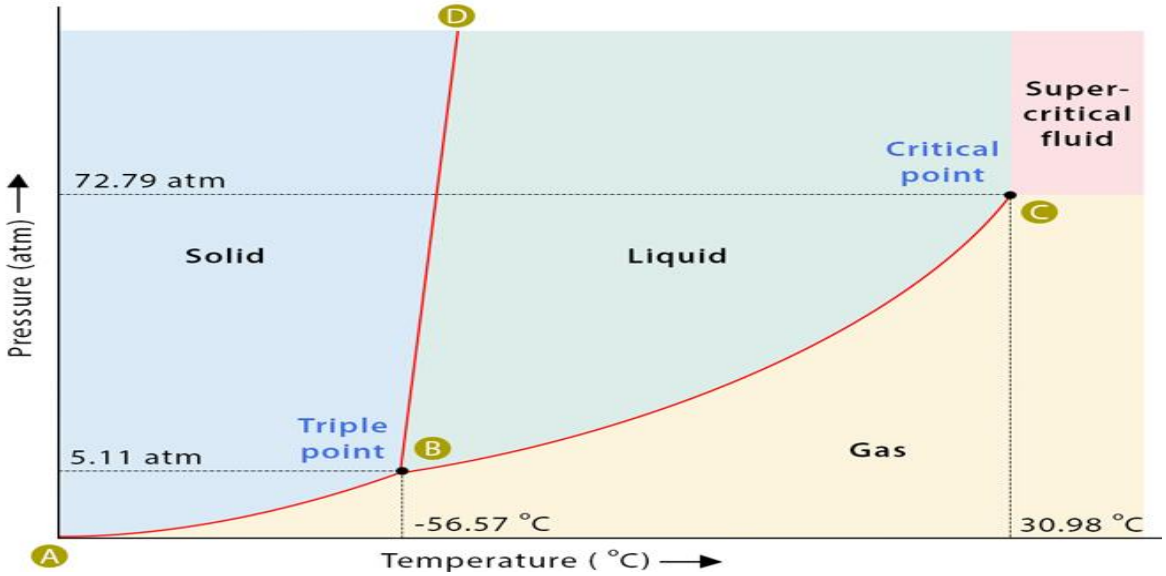

Figure 2.1: The carbon dioxide (CO_2) phase diagram [13].

It is significant to highlight that in non-thermodynamic systems, where the temperature is not a factor, phase transitions can occur and are described. Topological (structural), dynamic, and quantum phase transitions are a few examples. At the phase transition point (for instance, boiling point), the two phases of a substance, liquid, and vapor, have identical free energies and therefore are equally likely to exist. Below the boiling point, the liquid is in the more stable state of the two, whereas the gaseous form is preferred above [14].

Figure 2.1 is the carbon dioxide (CO_2) phase diagram. It has a sublimation curve (AB), a vaporization curve (BC), and a melting curve (BD). The triple point is located at Point B, where the temperature and pressure are -56.57 °C and 5.11 atm, respectively. It represents the pressure and temperature at which a material may coexist in all three phases. Point C is called the critical point, which denotes the maximum temperature (30.98 °C) and pressure (72.79 atm), beyond which it is impossible to discriminate between the liquid and gaseous phases. BC is the saturation curve of carbon dioxide to change from the liquid phase to the gaseous phase.

2.3 Superheated Liquid

In a rapid expansion of a pressurized liquefied gas toward atmospheric pressure, the substance could cross the saturation line without undergoing a phase transition [15]. The development of bubbles may be suppressed if there are no suitable nucleation sites. The liquid then reaches a high temperature (or metastable state). From this state, due to rapid depressurization, the liquid could expand vigorously without changing its phase. So, under saturation, the liquid becomes superheated if the pressure is decreased. Figure 2.2 shows a graphical representation of superheated liquid and metastable regions.

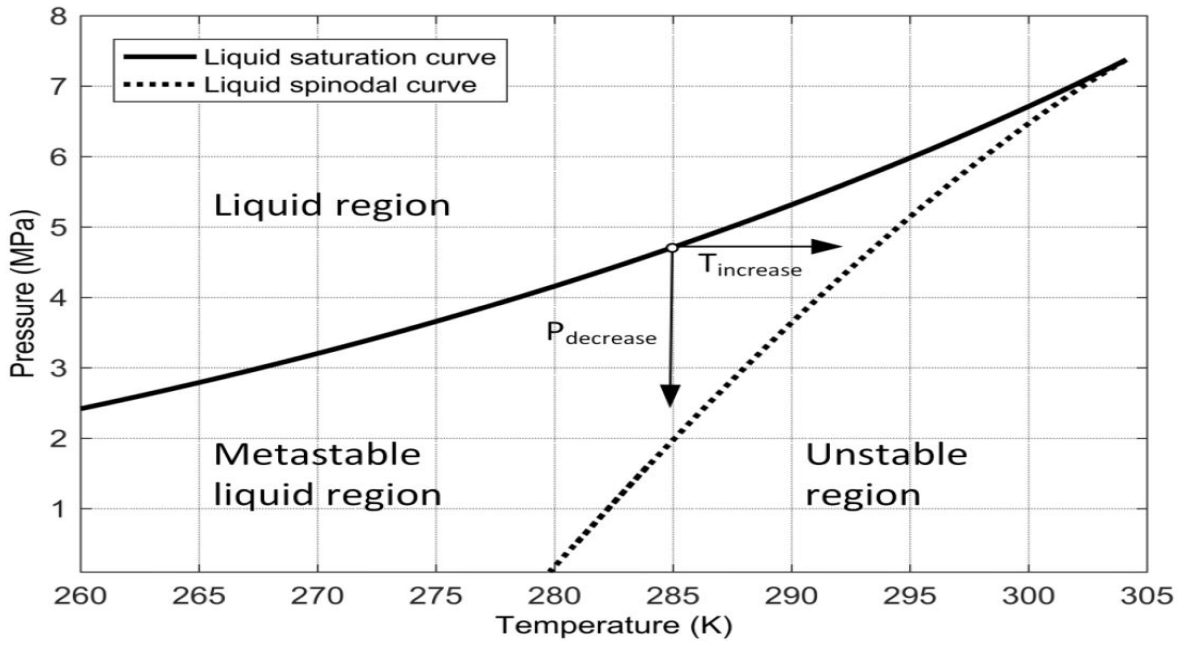

Figure 2.2: p-T diagram of carbon dioxide of Liquid Saturation and Spinodal Curve[16].

A superheated liquid is a particular case of a metastable system supersaturated with respect to the phase equilibrium condition defined by the equality of chemical potentials of the phases at given temperature and pressure values [17]. The superheat phenomenon occurs when a system passes the line of liquid-vapor equilibrium Ts(p), where Ts is the saturation temperature. P is the pressure without passing through a phase transition. In this view, a superheat first precedes and then follows boiling up, which is a superheated liquid's natural relaxing process. The characteristic values of a spatial scale (r_c) and a temporal scale (τ), the

so-called critical radius and lifetime of a system, respectively, serve as additional parameters of a thermodynamic description of superheated liquids [15].

The degree of superheat determines how serious the process is. There is a limit to how much superheat a metastable liquid can endure. This limit can be examined from either a thermodynamic or kinetic nucleation theory [18]. A liquid can only be heated far beyond its usual boiling point before a phase change occurs. The liquid's thermodynamic state is on the phase boundary between the metastable and thermodynamically unstable states at this theoretical maximum temperature. The spinodal curve, or border, separates intrinsically stable states concerning tiny perturbations in specific intrinsic variables from stable ones [19]. For a pure liquid, the spinodal curve, or thermodynamic limit of superheat, is defined by states for which $(\partial P/\partial V)_T = 0$. On the p-V diagram, an isotherm's slope is zero at its intersections with spinodal curves, as shown in Figure 2.3. The thermodynamic superheat limit, or TSL, is the temperature at which the liquid spinodal curve intersects.

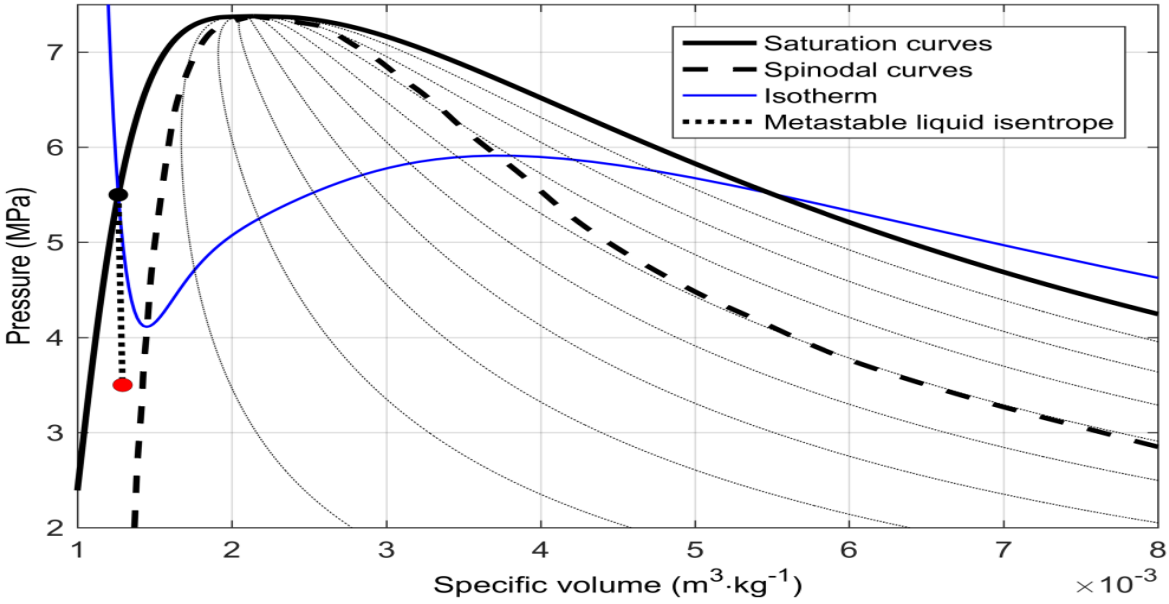

Figure 2.3: p-V diagram of carbon dioxide. The diagram shows the saturation curves, the spinodal curves, an isotherm, and a metastable liquid isentrope [16].

The temperature at the intersection with the liquid spinodal curve can be referred to as the thermodynamic superheat limit or TSL [20]. The cubic equation of state (EOS) can be used to predict the TSL by applying the criterion for the spinodal state. However, the correlations between P-V-T in an EOS are developed for equilibrium conditions and do not usually

extrapolate well into the metastable region[18]. For instance, using the Van der Waals equation of state, Spiegler et al. [21] derived the condition of mechanical stability i.e., the thermodynamic superheat limit, T_{TSL}, as

$$T_{TSL} = 0.844T_c \tag{2.1}$$

Lienhard [22] proposed the following correlation factor for the high-pressurized fluid for the thermodynamic superheat limit, T_{TSL}.

$$\left\{\frac{(T_{TSL} - T_S)}{T_C}\right\} = 0.905 - \left(\frac{T_S}{T_C}\right) + 0.095\left(\frac{T_S}{T_C}\right)^8 \tag{2.2}$$

T_C is the critical temperature (K), and T_S is the saturation temperature (K).

The second approach to describe the maximum liquid superheat temperature is called the kinetic homogeneous nucleation theory [23], [24] which bases bubble nucleation's temperature and pressure dependence on molecular fluctuation probability.

This treatment is based on kinetic nucleation theory and deals with probability and how rapidly the visible vapor bubbles form in a superheated liquid [18]. According to Xie [20], a superheat limit temperature that is determined by experiments will always be the KSL.

The theoretical framework of the kinetic theory of nucleation is employed to describe the process of nucleation in a superheated liquid. The phenomenon of nucleation involves converting a liquid state into a gaseous state. Superheated liquids are subjected to temperatures that exceed their boiling points, yet they persist in a liquid state due to the lack of nucleation sites.

At and above saturation conditions, the creation of critical nuclei can start the nucleation process. These nuclei are minute clusters of molecules with sufficient size to trigger the conversion of the liquid phase into the gas phase. The stochastic process of critical nuclei formation is subject to various influencing factors, including but not limited to temperature, pressure, and the characteristics of the liquid. There is a threshold nucleation rate at which the probability of a high bubble embryo formation rate is sufficient to transform the liquid to vapor.

According to the classical homogeneous nucleation theory, a liquid at a temperature T_l, the most considerable nucleation rate J, per unit liquid volume can be formulated [24], [25] as,

$$J(T_l) = N_l\, f\, exp\left(\frac{-W_{min}}{K_B T_l}\right) \tag{2.3}$$

Equation (2.3) presented in the text, uses various symbols to represent different parameters. Specifically, N denotes the number density of liquid molecules, f represents the frequency factor, k_B denotes the Boltzmann constant, and W_{min} denotes the free energy of formation of a critical nucleus.

Carey [26] derived the Equation for the homogeneous nucleation rate by simplifying it further.

$$J(T_l) = N_l \sqrt{\frac{3\sigma}{\pi m}}\, exp\left(\frac{-16\pi\sigma^3}{3K_B T_l\{P_s(T_l) - P_0\}^2}\right) \tag{2.4}$$

2.4 Significances of Homogeneous and Heterogeneous Nucleation in Term of Phase Change

There are two basic ways by which a new phase or substance forms in a system: homogeneous and heterogeneous nucleation.

In a homogeneous system [27], when the system's composition and properties are constant throughout, homogeneous nucleation describes the development of a new phase in material. This procedure involves spontaneous nucleation that doesn't involve any external surfaces or particles. Individual atoms, molecules, or ions are often clustered or aggregated to form a stable nucleus, which then expands to form the next phase. To break through the energy barrier for nucleation, homogeneous nucleation frequently needs circumstances such as strong supersaturation or supercooling.

On the other hand, heterogeneous nucleation refers to the creation of a new phase or substance on an outside particle or surface that is already existing in the system. Nucleation sites or heterogeneous nuclei are the names of these substances or surfaces. Because the energy barrier for nucleation is lowered by the existence of nucleation sites, heterogeneous nucleation is frequently more advantageous than homogeneous nucleation. Nucleation locations may

include imperfections, flaws, abrasive surfaces, or container walls. The atoms, molecules, or ions may absorb on the nucleation sites and form stable nuclei, which then expand to form the next phase, depending on whether the system is supersaturated or supercooled.

Heterogeneous nucleation requires less energy than homogeneous nucleation because the presence of the phase boundaries allows a lower interface area of the vapor embryo. Heterogeneous nucleation occurs at a lower degree of superheat than homogeneous nucleation [20]. In order for a BLEVE to happen, a significant portion of the liquid must evaporate quickly and that occurs certainly at the time of homogeneous nucleation. The evaporation started at moderate degrees of superheat process in the system by heterogeneous nucleation on a solid surface, on particle impurities, or inside microscopic gas cavities found on the solid surface. A very superheated state that is near to the liquid spinodal can be backed up by the restriction of heterogeneous nucleation. In close proximity to the thermodynamic superheat limit, homogeneous nucleation occurs. It differs from heterogeneous nucleation in that it occurs spontaneously in the liquid bulk and does not require a solid surface to form gas bubbles. The nucleation rates are found to be sensitive to small changes in conditions such as temperature and pressure [27]. The energy released when a liquid at its limit of superheat vaporizes could create a so-called vapor explosion if a significant fraction of this energy appears in the form of a thermal detonation wave or if bubbles grow at a rate that exceeds the ability of the surrounding liquid to acoustically respond [28].

The wave patterns and phase transitions that occur after a saturated liquid is rapidly depressurized are shown in the x-t diagram in Figure 2.4. A rarefaction wave (or fan) moves through the fluid as the initial shock wave moves outward. Behind the shock wave, a contact surface that initially distinguished between liquid and vapor is propagating. At a range of superheats close to the superheat limit, an evaporation wave can propagate behind the rarefaction fan through the metastable liquid [29].

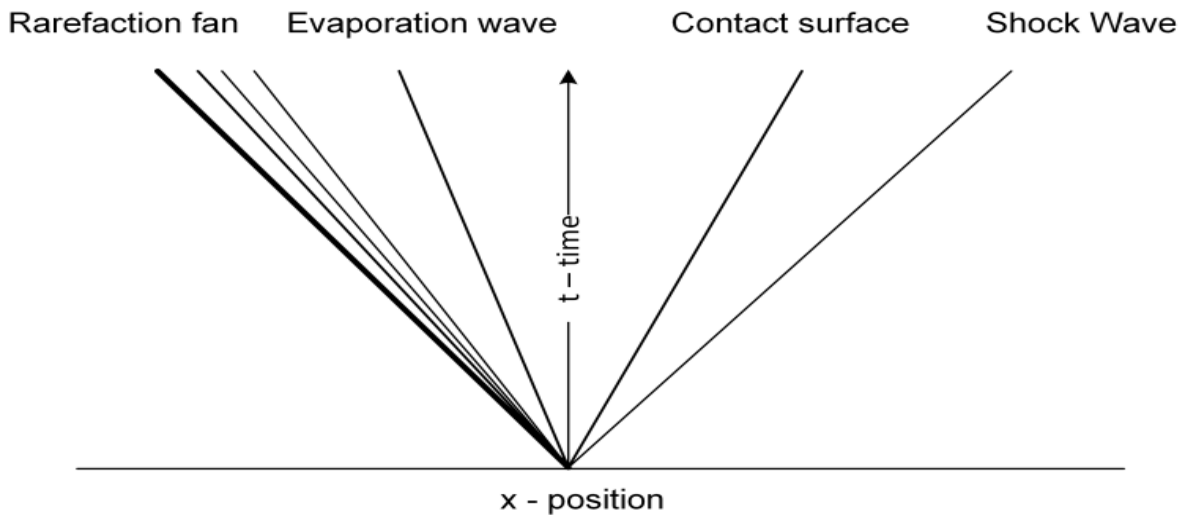

Figure 2.4: x-t diagram that illustrates wave patterns in rapid depressurization of a liquid. The diagram shows a shock wave; a contact surface; rarefaction wave, and an evaporation wave. Reproduced from Saurl [30].

2.5 Overview on BLEVE

The notion of "BLEVE" is introduced in this chapter along with relevant historical accidents. There has been a quick summary of the key hypotheses put up by different researchers regarding the mechanism and effects of BLEVE. Also given is more information about CO_2 BLEVE. The subsections provide a comprehensive overview of BLEVE, covering its definition, mechanism, repercussions (including pressure wave and fragments). In Section 2.5.3, the CO_2 BLEVE is discussed in more detail, along with its severity and the thermodynamics of CO_2 during an explosion.

2.5.1 Definition of BLEVE

BLEVE stands for Boiling Liquid Expanding Vapor Explosion. According to The Center for Chemical Process Safety, as cited in the work of Tasneem Abbasi et al [1], 'A BLEVE is a sudden release of a large mass of pressurized superheated liquid to the atmosphere'. The sudden release can be caused by failure of confinement, or 'Loss of Confinement (LOC)'. In the definition above, the term "pressurized superheated liquid" refers to a pressurized liquid gas in a superheated state, a thermodynamic state created when a liquid with a temperature higher than its boiling point experiences an abrupt depressurization.

2.5.2 The Effects of BLEVE

A PLG that is kept as a liquid/vapor mixture in a vessel that is suddenly opened or fails will quickly depressurize. The depressurization would almost immediately result in a two-phase flow splashing out of the vessel and almost certainly trigger a catastrophic explosion with harmful pressure waves and vessel pieces. The pressure waves produced by the boiling and evaporation of a PLG during depressurization may result in catastrophic effects. High-speed storage vessel pieces could be projected from the explosion center and seriously injure equipment and workers engaged in industrial operations. a BLEVE may lead to the following consequences, as described by Tasneem Abbasi et al [1].

1. 'Splashing of some of the liquid to form short-lived pools; the pools would be on fire if the liquid is flammable.'
2. Blast wave.
3. Flying fragments (missiles).
4. Fire or toxic gas release. If the pressured-liquefied vapor is flammable, as is often the case, the BLEVE leads to a fireball. If the material undergoing BLEVE is toxic, like ammonia or chlorine, there will be toxic gas dispersion.

2.5.3 Mechanism of BLEVE

There are few theories for the BLEVE process, which frequently rely on scant experimental evidence. Tasneem Abbasi et al. [1] have thoroughly explained the crucial processes involved in a typical BLEVE, described by Wei Ke [31] as follows.

1. Failure of the vessel. Various causes including overload heating, external hitting, or vessel corrosion may lead to a failure and sudden vessel opening.
2. Phase transition. When the vessel collapses, the pressure-liquefied gas held inside the vessel experiences rapid depressurization. When the original vessel pressure quickly drops to atmospheric pressure, the pressured liquid/vapor mixture, which was initially in a saturated thermodynamic state with a temperature greater than its boiling point, becomes superheated.

a) Bubble nucleation. The pressurized liquid can withstand being overheated when the temperature within the vessel is far below the liquid's superheat limit

temperature (SLT), which is explained in more depth later in this page and on the following page. Although quick bubble nucleation will begin internally if the temperature is higher than SLT, it will eventually result in a violent liquid/vapor mixture splashing out of the vessel and into the atmosphere.

b) Vaporization and Expansion. As the liquid boils, it undergoes a phase change from liquid to gaseous, forming a large volume of vapor. The vapor's rapid expansion creates a significant volume increase, leading to the formation of a vapor cloud.

c) Explosion due to depressurization and bubble nucleation. The boiling of the liquid followed by bubble nucleation, the expanding vapor from both the vaporization of the liquid and the initial vapor stored in the vessel, and the initial vapor stored in the vessel together will lead to an explosion (Boiling Liquid Expanding Vapor Explosion, BLEVE).

d) Blast wave formation. With an increase in the total volume of the expanding vapor, by a factor of a hundred to over a thousand-fold, a powerful blast wave will form and bring damage to facilities nearby.

e) Vessel rupture. Due to the powerful blast wave, the vessel ruptures and its pieces/fragments fly outwards everywhere like rocket missiles.

f) Fireball or dispersion of toxic fluid. The explosion caused by a BLEVE can lead to secondary hazards, such as flying debris, fireballs, and thermal radiation. These secondary hazards can cause further damage, injuries, and fires in the surrounding environment.

2.6 The Superheat Limit Theory as a Catalyst for the BLEVE

The known superheat limit theory, first proposed by Reid in [18] and [32] is the accepted theory of BLEVE. Figure 2.5 provides an illustration of the key concept. In these circumstances, the liquid and its vapor are in thermodynamic equilibrium inside the PLG vessel, and the pressure and temperature combination are at the saturation curve (points A or C). When a vessel ruptures, the pressure quickly drops, causing the liquid to become extremely hot. The amount of superheating that a liquid can endure has a limit. The superheat limit temperature is the greatest temperature a liquid can endure under constant pressure without going through a phase transition, while the superheat limit pressure is the lowest pressure at which a liquid can continue to be in its liquid state. The superheat limit curve is shown as the dashed line in Fig.2.1. As per the Reid theory, The vessel

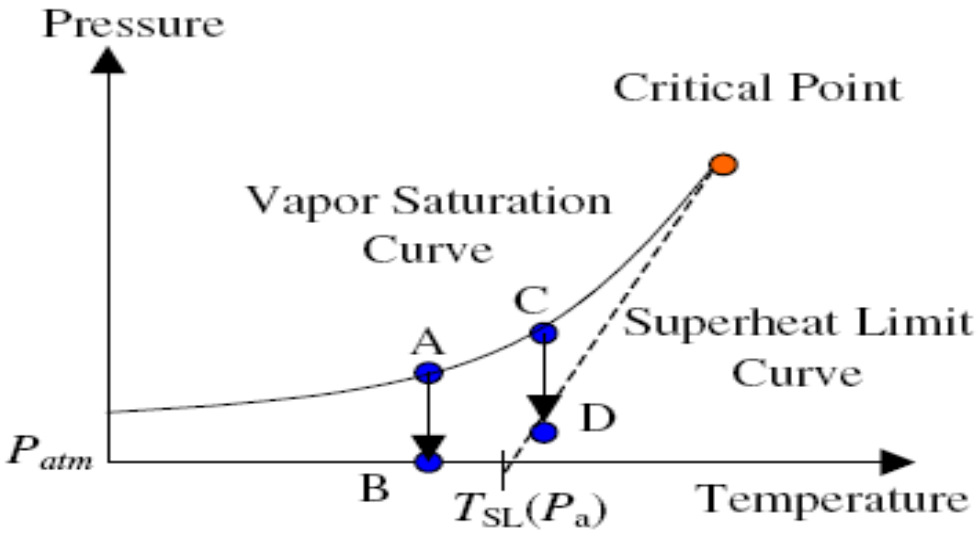

Figure 2.5: Schematic explanation of Reid's superheat limit theory for BLEVE in depressurization processes [33].

initially holds both pressured vapor and liquid in a saturated state prior to failure. When the vessel suddenly opens, the depressurization process begins. According to Figure 2-1's paths from point A to point B or point C to point D, this opening process is anticipated to go so quickly that the saturated temperature is assumed to remain constant. There are a total of two alternative pathways for the depressurization process under this isothermal assumption.

The first path occurs when the temperature is initially quite low at the start of depressurization, as point A's pressure decreases to atmospheric pressure before moving to point B. This depressurizing process resulted in the violent boiling of liquid. A BLEVE will not take place since the superheat-limit curve (the dotted line) has not yet been achieved.

The second method is taken when pressure descends to atmospheric pressure through point D, and the initial temperature is higher, as in the case of starting from point C when the temperature is initially higher. Since point D in this scenario crosses the superheat limit curve, an explosion is anticipated to happen, a BLEVE will take place.

Reid's "Superheat Limit Temperature" idea is based on the basic premise that a fluid's superheat limit temperature is the temperature at which a BLEVE occurs. Some BLEVE researchers have backed the theory. However, Prugh [5], [34] noted that a BLEVE can also happen when the two-phase mixture's initial temperature is lower than the superheat limit temperature. He said that one distinction between BLEVEs that occur at such low temperatures and those that do so at beginning temperatures higher than SLT is that the former's blast wave's (explosion energy) TNT equivalent is far smaller than the latter. It is considered that the SLT theory holds true for other fluids as well because it has been examined and verified with various fluids.

‘When it comes to pressurized liquefied gas, a substance that would be in gaseous state at atmospheric pressure but is held as liquid in a pressurized container, the SLT theory seems to be implicit. Numerous industrial chemicals such as liquid petroleum gas, compressed natural gas, liquefied chlorine, etc. have confirmed this theory, and so does superheated water in a boiler.’[35]

In their article, Tasneem Abbasi et al. [35] provided an example with ammonia, chlorine, and butane along with an examination of the degree of superheat. In the event that vessels containing these PLGs unintentionally rupture at 308 K or 350 K, they have computed the available degree of superheat. They used Figure 2-2 to illustrate the outcome. Additionally, the three PLGs' pressure-temperature curves and accompanying superheat limit curves (tangents drawn from critical points) are shown in the image. The values of boiling point (BP) and superheat limit temperature (SLT) at 1 atm for ammonia is 239.8 K and 347.21 K

respectively. For chlorine, BP = 239.1 K, SLT = 247.22 K. For butane, BP = 272.7 K, SLT = 362.61 K. The different available degrees of superheat with different temperature of rupture (initial temperature) for these three PLGs are indicated in Figure 2.6.

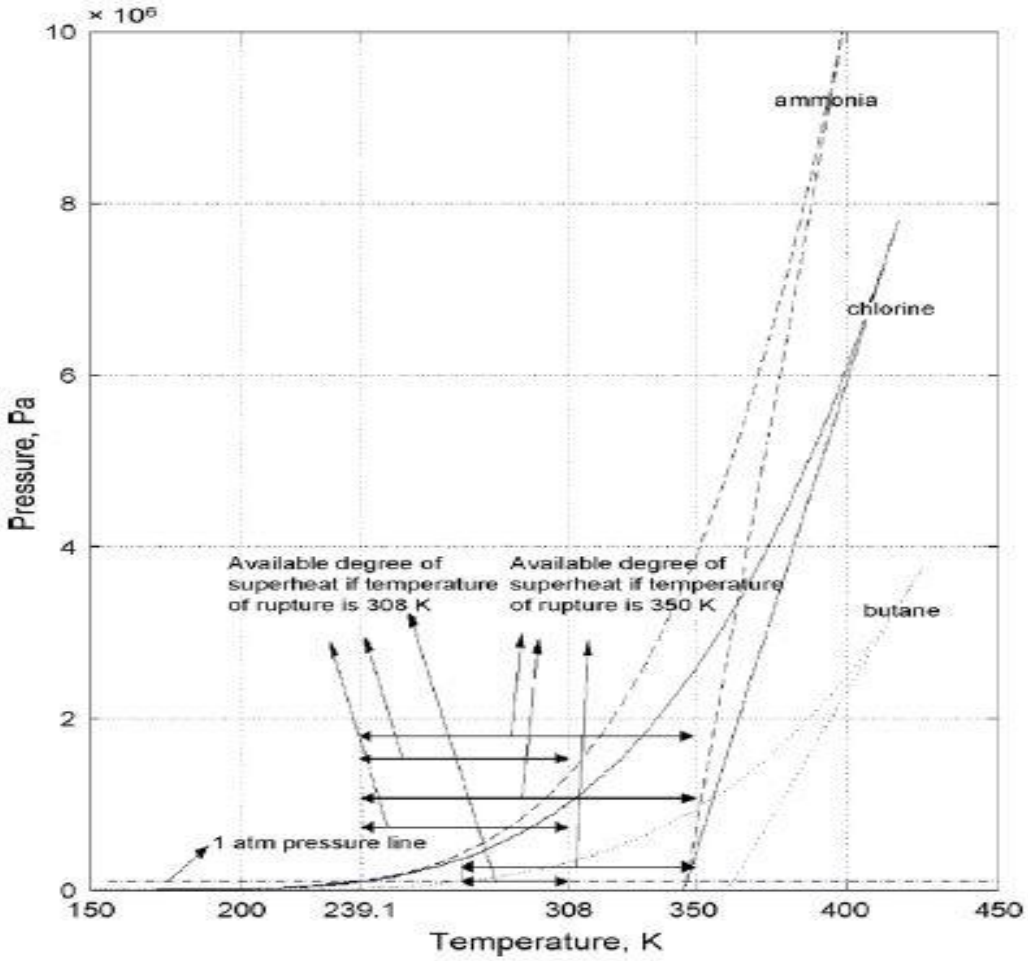

Figure 2.6: Pressure-temperature curves and superheat limit curves for ammonia, chlorine, and butane, with degrees of superheat at two rupture temperatures (308 K/350 K) [33].

The assumption made in their experiment in relation to the degree of superheat is that the temperature differential determines the intensity of the blast wave produced by an explosion. A BLEVE would be more likely to happen the more superheat is available for a pressurized liquefied gas in a storage vessel.

Seven approaches to determining the superheat limit temperature of 22 compounds were examined by Salla et al. [36] in their study. Based on the energy balance in the initial liquid mass shortly prior to the explosion, an estimated TSL in CO_2 was T = 289.7 K.

The TSL in CO_2 was estimated by Abbasi and Abbasi [33] using data from many different sources of EOS. The estimations ranged in size from 257 to 283 K. The same authors reported an experimental temperature measurement of T = 267 K. The kinetic superheat limit (KSL) is predicted by this estimate.

The superheat limit theory states that keeping the CO_2 below T = 267 K could prevent a BLEVE from happening during a rapid depressurization. The saturation pressure at this temperature is P = 3.0 MPa. Investigation reports from previous tank explosions show only partial agreement with this hypothesis. The findings after the explosion in Worms concluded that the tank pressure was between 3.5 - 5.1 MPa. This pressure corresponded to a saturation temperature in the range of 273 - 288 K at the time of rupture [9].

Although the storage temperatures were stated to be 258 K and 233 K, respectively, the accident reports from Yuhang [10] and Repcelok [37] show that a BLEVE might still happen even if the beginning temperature is below the superheat limit temperature [10]. In their studies using small-scale CO_2 BLEVE tests, Bjerketvedt et al. [8] and Ke [31] provided evidence in support of this hypothesis. In these tests, the starting temperatures were below the superheat limit at 1 atm. In fact, Birk et al. [2] questioned whether homogeneous nucleation even played a part in the development of BLEVEs. From their experimental work with 40-liter CO_2 cylinders, Van der Voort et al. [38] deduced that BLEVE blasts did not vanish abruptly below the homogenous nucleation temperature but instead displayed a steady decrease. These earlier findings imply that a BLEVE may not exclusively be caused by homogeneous bulk nucleation at the superheat limit. Always take precautions to avoid potentially dangerous situations like overfilling, abrupt pressure drops, and operation at temperatures above or below the material specification limits.

2.7 Vaporization Dynamics of a BLEVE

In a BLEVE (Boiling Liquid Expanding Vapor Explosion), the rapid release and vaporization of a liquid is caused by a series of intricate events that take place when a pressurized vessel holding the liquid abruptly ruptures. The severity and characteristics of a BLEVE incident are greatly influenced by these processes. It's crucial to keep in mind that the vaporization dynamics of a BLEVE are extremely complex and rely on a number of variables, including

the liquid's characteristics, the pressure inside the vessel, the vessel's structural integrity, and the external environmental conditions. Xie [20] provides an explanation for this possession as in a practical BLEVE, pressure decreases in the liquid as a wave, with local temperatures varying depending on accident features and the heat used for vaporization. The situation in a real incident is more complex than simple trajectories. Starting points at different locations on the saturation curve may be different, and pressure decreases can be stopped by expanding the mixture and controlling the rate of depressurization.

When a liquid is superheated but is still far away from the superheat limit, vaporization will start first in locations most favorable for the formation of initial small bubbles which is on solid surfaces or on dust or other solid particles in the fluid. Once bubbles are formed, they grow according to growth laws which have been well-studied in the literature [39], [40].

Smaller bubbles (nuclei) are produced differently when the superheat limit state is being approached than when it is being avoided because they do so more quickly and uniformly within the fluid. The smallest stable bubbles are substantially smaller near the KSL than they are elsewhere. To explain this situation, the traditional homogeneous nucleation theory has been devised. It turns out that the accuracy of its forecasts of the nucleation rate depends greatly on the specifics. To remedy This, De Sá et al. [41] and Delale et al. [42] offer different formulations of the theory. The growth of bubbles at the superheat limit also proceeds in a different manner than away from the superheat limit [43].

The quick bubble expansion could lead to a pressure increase that would balance the initial pressure decrease and prevent the liquid from exceeding the superheat limit. The evaluation of the impacts of quick depressurization or rapid heating must take this phenomenon into account. It is unrealistic to believe that when a vessel bursts, its contents "instantaneously" exceed atmospheric pressure or the superheat limit curve. This has been considered in modifying the superheat limit idea put forward in [44]. According to the review's executive summary[45] in [44], homogenous boiling only takes place at the spot where liquid pulled out of the breach first reaches atmospheric pressure. Before the vessel might completely disintegrates, their research focuses on the liquid behavior inside the vessel (liquid hammer, pressure recovery, etc.).

These arguments suggest that in addition to experiments and thermodynamic models, fluid dynamic models and experiments are also necessary to estimate the propagation speed of vaporization fronts to determine the superheat limit curve for diverse substances.

A vapourization front can have a very complex shape and wildly fluctuating properties. The breakup of existing bubbles into smaller bubbles in a wildly fluctuating vaporization front creates extra area and new nuclei for heterogeneous vapourization. This can enhance the vapourization rate and the front propagation rate enormously. The question arises whether the vapourization in a propagating front can generate a sufficiently strong volume source for significant blast propagation.

2.8 Single Vapor-Bubble Nucleation and Growth

Rapid vaporization is necessary for BLEVE creation. Vaporization has begun by the nucleation of tiny bubbles, which is followed by the expansion of these bubbles. It is necessary to distinguish between bubble expansion and nucleation in a meta-stable state, the KSL is still far away, and nucleation and vaporization are occurring nearby. Homogeneous nucleation is far less likely to occur in non-KSL settings than heterogeneous nucleation, and the availability and characteristics of surfaces for nucleation are also factors in the question of how quickly a nucleation occurs. Experimental studies on the bubble growth process at the superheat limit are described in [46]–[50].

Lesin et al. [47] express in their study, in contrast to the smooth bubbles in traditional boiling, the liquid-vapor interface in a vapor explosion process exhibits a large-amplitude small-scale roughening during the majority of the evaporative stage. They observed that the bubble was Rayleigh-Taylor unstable and disintegrated into a cloud of tiny bubbles.

A model for the dynamic behavior of a single liquid butane droplet boiling explosively near its superheat limit was created and examined by Lesin et al. [46].

Results from an experimental setup using a bubble column were presented by Moore [51]. The test liquid could reach a highly superheated condition, and there were no nuclei that could create bubbles. The fundamental ideas outlined by Reid [18] are illustrated in Figure 2.7. A host fluid that is immiscible with the test fluid is put inside a vertical glass column. The

column is heated to a temperature difference between the top and bottom that is noticeably greater. A test fluid droplet with a diameter of roughly 1 mm is injected into the bottom of the column using a syringe. Because it is less dense than the host fluid, the droplet rises. The host liquid simultaneously transmits heat to the test liquid while maintaining a steady pressure. The temperature rises as the droplet ascends toward the top of the column. The droplet erupts violently when it reaches the homogeneous nucleation temperature (KSL) at a certain height. This method, which uses isobaric heating to measure the superheat limit temperature, has demonstrated remarkable reproducibility for the same test fluid in various columns [18].

Shepherd's work on the rapid evaporation of droplets at the superheat limit was continued by Frost [50] and Frost and Sturtevant [49] Tests on pentane, isopentane, and ether—three additional fluids—confirmed the generality of Shepherd's observations. The range of 0.025 to 0.45 MPa was used to study the impact of ambient pressure. The fact that the vaporization rate fell as ambient pressure increased was an intriguing finding. The reason given was that when pressure increased, the degree of superheat attained at the superheat limit decreased.

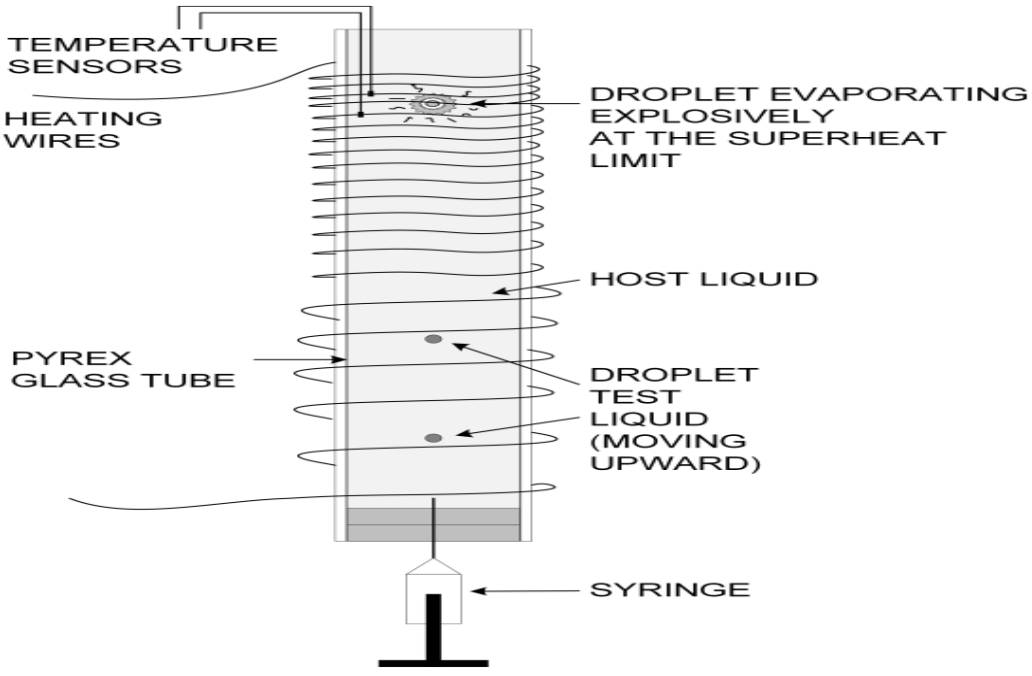

Figure 2.7: Schematic of a bubble column setup that measures the superheat limit temperature of droplets at constant pressure. Reproduced from Reid (1976) [18].

A model that predicts the mass transfer flux in rapid evaporation near the superheat limit was presented by Nguyen et al. in [52] . The model's application to the case of a butane droplet

was contrasted with Shepherd and Sturtevandt's [47] research. The writers claimed that "general agreement" existed between the simulation and measurement results. Park et al. [53] measured the superheat limit temperature of four pure hydrocarbons, which included pentane, hexane, cyclohexane and benzene, and a selection of binary mixtures.

2.9 Evaporation Waves and Boiling Front Propagation

The words "evaporation waves" and "boiling front propagation" relate to specific phenomena that happen during the vaporization of the superheated liquid inside the ruptured vessel in the context of a BLEVE (Boiling Liquid Expanding Vapor Explosion). The quick vaporization process and the explosion that follows depend heavily on these dynamics.

Evaporation Waves: During the early phases of a BLEVE, a specific category of pressure wave called evaporation waves develops. The superheated liquid inside the ruptured pressure vessel starts to evaporate quickly. The process of vaporization generates a shock wave that returns into the liquid that is still there and prompts additional localized rapid vaporization in a wave-like pattern. An evaporation wave is the name for these phenomena. These waves keep moving through the liquid that is still present, creating a cascade effect of vaporization that results in the practically instantaneous emission of a significant amount of vapor. The evaporation wave can increase the energy release and the damage potential of a BLEVE [54].

The border or interface between the liquid and vapor phases inside the vessel is referred to as the boiling front. The boiling front is a movable boundary that forms during the BLEVE as the evaporation waves pass through the liquid region. Rapidly moving across the liquid, this front causes the liquid to evaporate. The characteristics of the liquid, the pressure, and the size of the vessel are only a few of the variables that affect how quickly the boiling front advances.

The vapor cloud that emerges following the BLEVE event expands quickly due to both boiling front propagation and evaporation waves. The explosive force that distinguishes a BLEVE is produced by the abrupt release of a significant amount of vapor and the corresponding energy release.

Instead of being heated at constant pressure, the liquid is now subject to rapid depressurization. After the initial rupture, a rarefaction wave propagates through the saturated

liquid. If heterogeneous nucleation is suppressed, the liquid becomes superheated. A phase change process happens behind the initial depressurization. The phase change can under certain conditions be restricted to a narrow region called an evaporation wave that is traveling through the expanded metastable liquid state at a nearly constant velocity [29]. Figure 2.8 shows a simplified illustration of a rapid depressurization and evaporation process. The evaporation wave can be thought of as a transition between a superheated liquid state and an equilibrium liquid-vapor state. According to Hill [55], this analysis is analog to the investigation of propagating deflagration waves described in premixed combustion studies.

The liquid in the metastable area becomes extremely superheated when a pressurized liquid of CO_2 rapidly decompresses inside a vertical tank with smooth sides. During evaporation, homogenous nucleation occurs in the liquid bulk, and the liquid subsequently releases its internal energy. A portion of the liquid begins to evaporate, and heat is removed from it in the process.

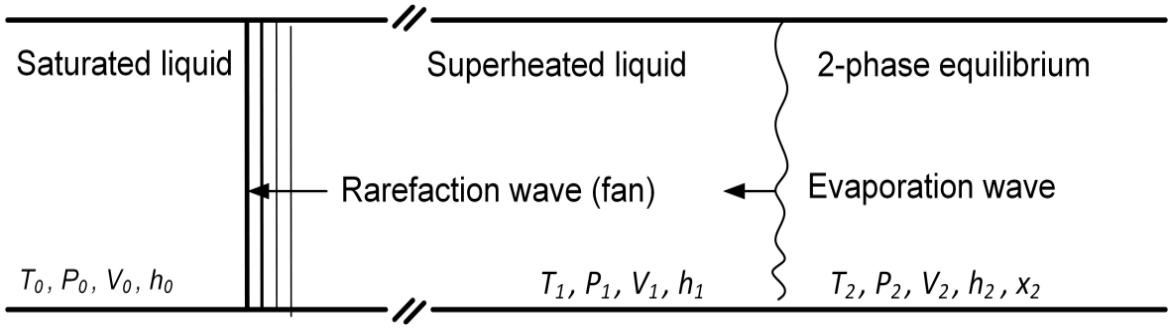

Figure 2.8: Illustration of an evaporation wave propagating into a superheated liquid [56].

The liquid's temperature and vapor pressure consequently decrease. When the liquid hits the boiling point, the temperature of the liquid starts decreasing. The vapor pressure also drops simultaneously toward atmospheric pressure. The rapid phase change with expanded vapors' volume results in multiple phases bursting out of the vessel, and, subsequently, generates a shock wave due to compression of the surrounding air [32]. A primary vapor-liquid contact surface is established, and this wave rapidly spreads upward to the surrounding area. Following the pressure drop, an evaporation wave is followed by an accelerated rarefaction wave that travels lower inside the vessel. The evaporation wave could exemplify a limited zone where the phase transitions occur and travel with almost constant velocity [29]. When the temperature approaches the superheat limit, the evaporation wave may be promoted into

a metastable liquid depending on the degree of superheat. When the superheat degree is low, the subsequent evaporation rate is insufficient to generate a severe explosion [37]. Figure 2.9 shows an x-t diagram of the depressurization and phase change process with more details than the diagram presented in Figure 2.4.

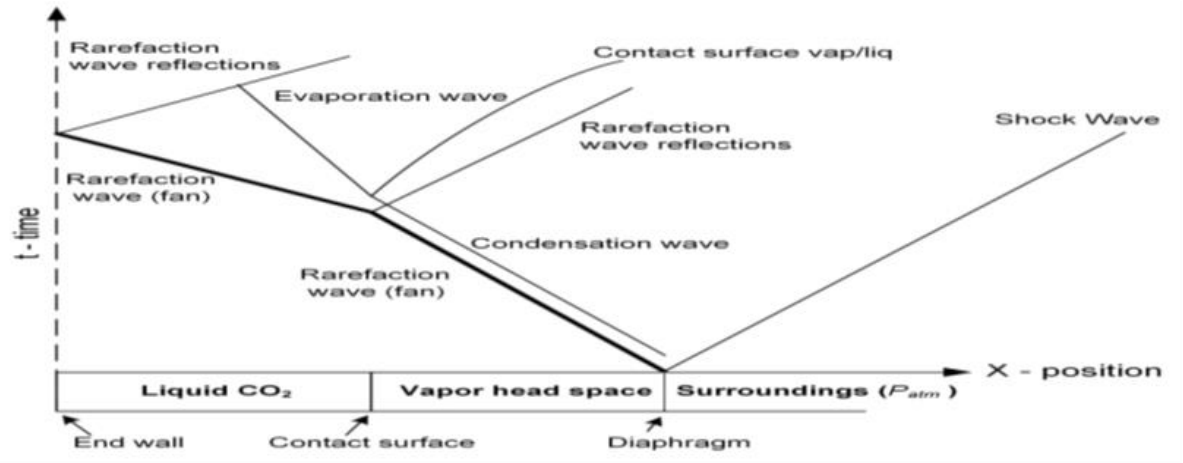

Figure 2.9: x-t diagram of depressurization and phase change processes in a channel that is filled with a pressurized liquefied gas and sealed with a diaphragm [56].

2.9.1 Experimental Study Evaporation Waves

In a recent experimental study on Evaporation characteristics in an upward conical vessel's three different regions, Ibrahim et al. [19] presented that the evaporation wave velocity increases downward with decreasing cross-section and increased liquid volume fraction. The thermodynamic properties of superheated CO_2 in the metastable state were determined utilizing the Span-Wagner equation of state. They calculated the highest and lowest velocities of evaporation wave were 111.6 and 37.8 m/s in the region close to the vessel's bottom and upper region, respectively, for 96.4% LVF. The study also reported that "Expansion waves velocities varied in different vessel regions while they were nearly constant for the duct. The evaporation wave velocities were nearly identical for the duct and the upper conical vessel's regions". Their study was based on pressure records.

Das et al. [57] report experiments on boiling propagation in a suddenly depressurised superheated vertical column filled with water. The velocity of boiling front propagation (BFP) is found to depend strongly on liquid superheat, liquid purity, and test section size. They concluded that the boiling front velocity increased with increased degree superheat and test

section diameter. Using a similar configuration, several other authors have succeeded in identifying the key properties of evaporation fronts [58], [59] [29].

Simões-Moreira and Shepherd [29] observe the range of conditions in which evaporation waves occur: "There were also definite limits of minimum and maximum superheats for which we reliably observed evaporation waves. Outside these limits, nucleation upstream of the wave would disrupt our observations. At low superheats, the evaporation wave was slow and there was a long dwell time before the onset of the wave. This required metastable fluid to be in the test cell for a long period of time, and heterogeneous nucleation would occur. At moderate superheats the wave would start promptly and move quickly enough that heterogeneous nucleation upstream of the wave would not occur. At high superheats, the nucleation rate became so high that despite high evaporation wave speeds, heterogeneous nucleation occurred upstream of the wave."

Ciccarelli et al. [60] presented a study on the rapid boiling of CO_2 The study investigated depressurization from a 16mm inner-diameter polycarbonate tube (driver section) partially filled with CO_2 liquid, expanding into a similar diameter tube (driven section). The tubes were separated by an aluminum diaphragm, and the temperature was maintained at 10°C. They concluded that Contact surface motion generates compression waves, impacting the post-shock pressure profile; rapid evaporation doesn't affect driver expansion. Tosse [61] demonstrated rapid boiling of pressurized liquefied CO_2 in a polycarbonate tube, revealing evaporation waves with a 20-30 m/s velocity.

Hahne and Barthau [62] observed evaporation waves in adiabatic flashing processes with low superheat and small depressurization rates. They also found that the presence of metal/liquid contacts decreased the necessary superheat for the formation of evaporation waves.

2.9.2 Simulation of Explosive Evaporation

Simulation work was done by van der Voort et al. [63] to demonstrate the experiment setup involved evaporating 40 liters of CO_2 using a cylindrical source area with an 11cm radius and 110cm height on Earth's surface has been simulated by assuming cylindrical symmetry. The volume of the source area and surrounding space was meshed using a two-dimensional mesh.

The pressure distribution around the evaporating CO_2 was modeled using color shading and isobar lines in figure 2.10. Where the isobar lines accumulate, revealing shock phenomena.

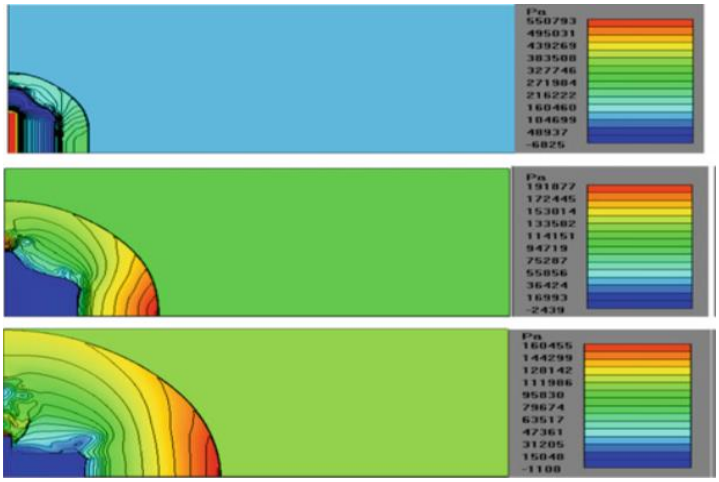

Figure 2.10: Pressure distributions produced by the explosive evaporation of 40 l of liquid CO_2 at a temperature of 290K [63].

A blast flow field expands, leading to a shock, which connects the overpressure in the blast wave and under pressure around the source. The shock propagates up the supersonic expansion flow of CO_2, driving it outward. As outflow velocities decrease, the shock moves upstream, focusing and reflecting, and becoming the origin of a secondary blast wave. The evolution of overpressure has been recorded at 1, 2 and 3m distance from the bottle axis at a vertical position of 0.7m above the earth's surface [63]. The records are presented in Fig. 2.11.

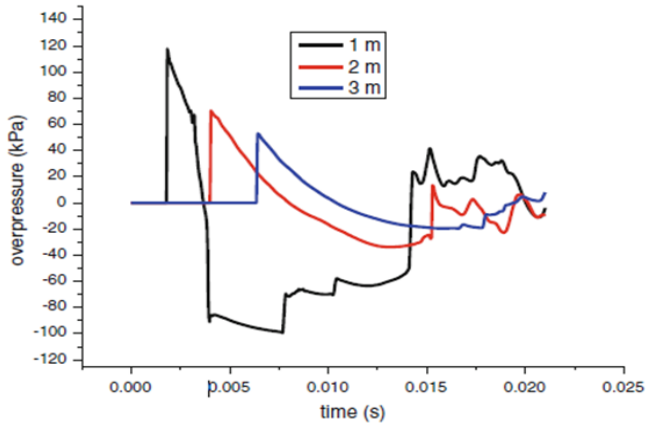

Figure 2.11: Overpressure–time developments recorded at 1, 2 and 3m distance from the axis of the cylinder and at height 0.7m, calculated in a two-dimensional mesh of cylindrical symmetry around a source area initially containing 40-liter liquid CO_2 at 290 K [63].

2.10 BLEVE Research

The experimental investigations that describe the small and medium-scale BLEVE tests are introduced in this section. The investigation of the applicability of the rapid depressurization and superheat limit theory was a common driving force in most investigations.

Kim-E (1978), and Kim-E and Reid (1983) performed a series of rapid venting experiments with pressurized liquefied CO_2 in a 7-liter vessel. The motivation for the study was to validate the superheat limit theory as a trigger for a BLEVE. None of the thirteen experiments resulted in a vessel rupture. An explanation offered for the discrepancy between theory and experiments was the occurrence of heterogeneous nucleation on the wall or plunger rod. Another explanation was that the reflected shock resulting from the breaking of the burst disc led to vapor formation in the partially superheated liquid.

2.10.1 Birk et al. Experiment

Birk et al. [2] analyzed blast overpressures from 20 propane tank failures and BLEVE, finding that liquid energy content does not contribute to shock overpressures in near or far fields. They found that shock overpressures could be estimated from vapor energy alone for all tests, even for liquid temperatures below, at, and above the atmospheric superheat limit for propane. Birk et al. [2] point out that the expansion of the flashing liquid contributes to other hazards such as projectiles and close in dynamic pressure effects and conclude "Of course BLEVE releases in enclosed spaces such as tunnels or buildings have different hazards." Birk et al. [2] also make the remark that the occurrence of a double-pressure peak should not be interpreted as proof of a liquid vaporization generated second blast wave (after the first one generated by the expansion of the vapor space) but is a well-known effect in explosions by gas expansion.

2.10.2 Bjerketvedt et al. Experiment

Bjerketvedt et al. [38] carried out a series of small-scale BLEVE tests in transparent cylindrical plastic tubes. The cylindrical tubes containing CO_2 are 60mm or 100mm in length and the outer diameter is 40mm. Solid CO_2 is first put in the vessel, and after heating and pressurization, CO_2 reaches the saturation state at the pressure of 3 to 4.5 MPa. The internal pressure increased until the tubes ruptured at pressures between 3 - 4.5 MPa. A high-speed

video camera with a frame rate of 10000 frames/sec is used to record the rupture of the tube, the projection of fragments and the formation of CO_2 cloud around the ruptured tube. The authors proposed that the decompression of the vapor phase generates shock waves in the experiments. Bjerketvedt et al. compare the measured shock waves with the modeled shock waves generated by the expansion of the compressed vapor CO_2 only (without the boiling of the liquid CO_2) and find the agreement is quite well. Therefore, they conclude that "the shock front is governed by the expansion of the gas phase (vapor) in the vessel prior to explosion" in their experiments.

2.10.3 Van der Voort et al. Experiment

Van der Voort et al. [38] conducted modeling and experimental work with 40- liter CO_2 cylinders. The overpressures from the experiments were measured and compared with simulations. Modeled results were conservative (produced higher overpressure) compared to the experimental results. The model assumes that the explosive evaporation process is limited by the inertia of the expanding liquid/vapor mixture into the surroundings. BLEVE experiments performed at initial temperatures both above and below the superheat limit temperature showed that BLEVE blast did not abruptly disappear below the SLT but followed a gradual decay. The results showed that low CO_2 storage temperatures should not exclude BLEVE scenarios from hazard assessments.

2.10.4 Wei Ke Experiment

Wei Ke [31] thesis study on CO_2 BLEVE (Boiling Liquid Expanding Vapor Explosion) In this work, CO_2 BLEVE experiments have been performed in the laboratory. The main objective was to construct a functional experimental rig and to gain further knowledge on the mechanism and consequences of CO_2 BLEVE by analyzing experimental data. With the application of new knowledge gained, CO_2 storage risk in the industry may be further reduced.

2.11 BLEVE Simulation

Mishra K et al. [64] did an experimental investigation and CFD simulations to measure and predict fireball characteristics of a BLEVE using a peroxy-fuel which is represent in figure 2.12.

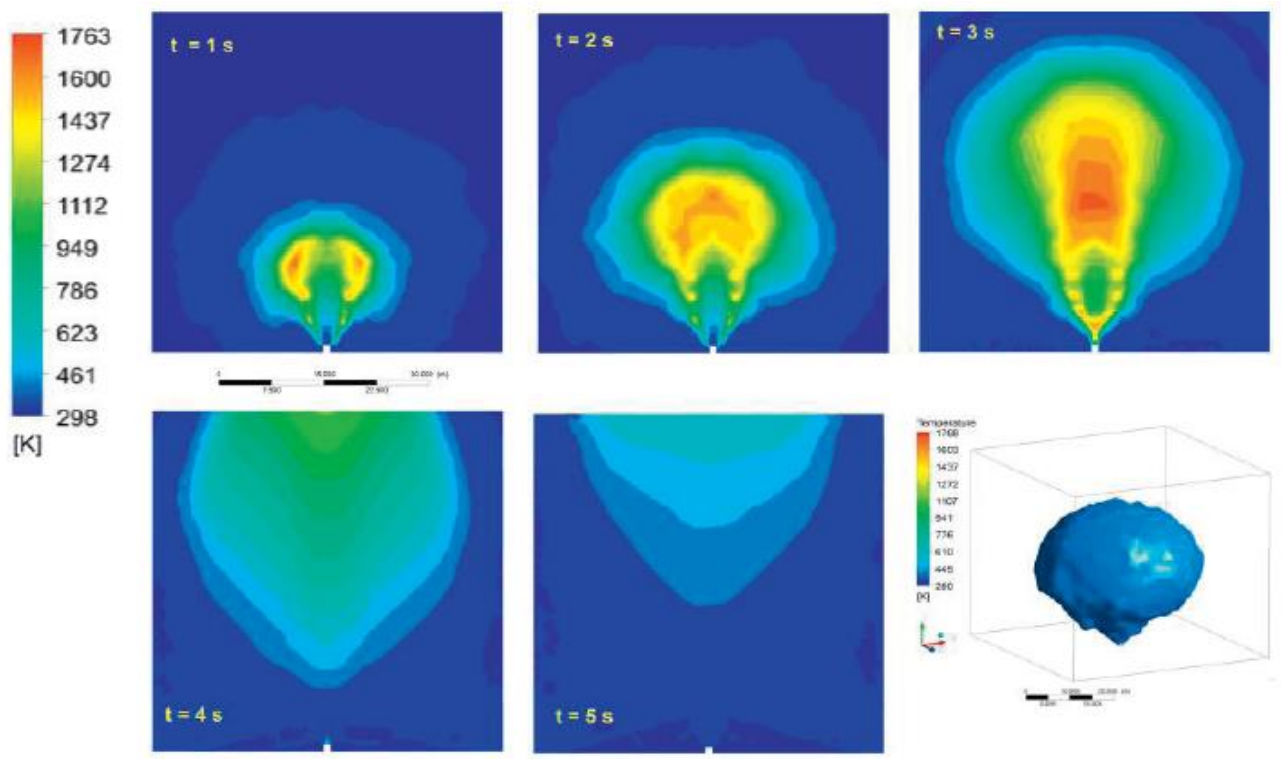

Figure 2.12: CFD predicted time evolution of a peroxy-fuel fireball (t = 1 s to 5 s are showing CFD predicts the outer flame surface temperature as 400K [64].

In the investigation, the 2.5-second release time and 25 m/s release velocity of fuel vapor were examined. There were sub-models for radiation, combustion, and turbulence. Runs for Jet A, propane, and peroxyfuel were transient. A peroxy-fuel flame that fully developed at 3 seconds and then dissipated was predicted by CFD to evolve. The outer flame surface temperature of 400 K corresponded to the projected temperatures.

2.12 Equations of State (EOS)

A thermodynamic equation of state or observations is needed to determine the attributes of a state and the transition. The state information is frequently extracted from an EOS since it is challenging to make accurate experimental observations in the metastable area. Extrapolation is required to derive state values in the zone of metastability because the majority of equations of state are often only valid under equilibrium conditions. The chosen EOS has an impact on the calculations.

In theory, any cubic EOS can be chosen to define the P-V-T relations for the fluid flowing through the metastable and unstable zone. The variance of the computed findings, however, can be substantial. Examples of EOS utilized in dynamic simulations of rapid depressurization and phase change include the stiffened gas Tosse [61] and Saurel [30]; van der Waal [61]; Peng-Robinson Stryjek-Vera [20].

The state of matter is described by state variables, such as temperature, pressure, and specific volume. Different states correspond to different values of state variables. An equation describing the relation between state variables in a wide range of states is called the equation of state. Equations of state have been widely used in describing the properties of pure fluids, a mixture of fluids and solids. The research on the equation of state started with gases. Based on Boyle's law in 1662 and Charles's law in 1787, the ideal gas law was first derived by Émile Clapeyron in 1834 and further developed to be

$$PV = nRT \tag{2.5}$$

where V is the molar volume and R is the universal gas constant, T is temperature, P is pressure, n is mole number of gas the ideal gas law ignores the molecular interactions in regarding the molecules as material points with zero volume (equivalent to ignoring the molecular repulsion) and neglecting the attracting force of the molecules. Those simplifications are acceptable for gaseous states because the specific volume is relatively large; therefore, the interactions between molecules are negligible. In liquid states, the molecular attraction and repulsion are not negligible, and in order to describe liquid states, the EOS has to be different from the ideal gas law. In this respect, the Stiffened Gas EOS has been widely used.

2.13 Helmholtz Free Energy Type Equations of State

When one has knowledge of the Helmholtz free energy function and its partial derivatives for a pure substance, one is able to determine any additional thermodynamic parameters that are of interest. Because of this, the Helmholtz free energy as a function of specific volume and temperature, denoted by the notation $f(v,T)$, is a form that is frequently used for multi-parameter equations of state such as the Span-Wagner EOS. This form gives rise to formulations for the partial derivatives. When formulating the Span-Wagner EOS, reduced dimensionless form is the method of choice. The Helmholtz free energy function can be used to compute a number of thermodynamic parameters in this thesis study by Matlab using thermodynamics-master code from GitHub[65], and Table 2.1 provides some of the thermodynamic parameters that can be obtained by the Helmholtz free energy functions[66].

Table 2.1: Different thermodynamic parameters formula given by the Helmholtz free energy function in terms of the partial derivatives of $f(T, v)$.

Thermodynamic parameter	**Symbol**	**Helmholtz formulation**
Pressure	p	$p = -(\partial f/\partial v)_T$
Entropy	S	$S = -(\partial f/\partial T)_v$
Enthalpy	h	$h = u + pv = f - Tf_T - vf_v$
Internal energy	u	$u = f - Tf_T$
Speed of sound	c	$c^2 = \frac{v^2}{M_w}(f_{vv} - \frac{f_{Tv}^2}{f_{TT}})$

3 Thesis Methodology

In this chapter the selection of an EOS has been discussed, the calculation of the properties in the metastable states from the EOS and the thermodynamics data acquire process of isentropic expansion from Matlab.

3.1 Why EOS is Required

The first ingredient needed in a model for a BLEVE is a thermodynamic equation of state (EOS). The main function of an EOS is to give the relation between the state variables like pressure, temperature, and specific volume in states of thermodynamic equilibrium. In the context of phase transition, it is necessary to use an EOS adequate for describing the two-phase mixture of a liquid and its vapor. And moreover, the EOS should also be adequate to describe the relation between state variables in a metastable state, out of equilibrium. Using the properties of the metastable state and using information from the vaporization model, the EOS will, for example, predict the change in temperature due to changes in the pressure and density of the mixture.

3.2 The Stiffened Gas Equation of State

When thinking about liquids under high pressures, the stabilized gas equation of state (SG-EOS) is frequently utilized. It is a variant of the ideal equation of state in which the correction factor P_∞ raises the pressure. The fluid that is already under pressure P_∞ and behaves as an ideal gas is under the control of the SG-EOS. To put it another way, the SG-EOS becomes the ideal gas EOS when P_∞ is equal to 0. The SG-EOS's constant parameters are as γ, ρ, and P_∞. A straightforward and convex formulation that can be used to simulate the thermodynamic behavior of liquids, gases, and mixes is the stiffening gas equation of state. It is predicated on the idea that pressure is a linear function of specific internal energy, specific volume, and various constants that depend on the physical characteristics of the material. The stiffening gas equation of state has the following general form:

$$P = (\gamma - 1)\rho(e - e^*) - \gamma P_\infty \tag{3.1}$$

where P is the pressure, ρ is the density, and e is the specific internal energy of the fluid. The parameters γ, e^*, and P_∞ are constants specific to the fluid. Herein, e∗ defines the zero point for the internal energy and becomes relevant when phase transitions are involved. The parameter P_∞ is infinite pressure which leads to the "stiffened" properties compared to ideal gases; a large value of P_∞ implies near-incompressible behavior. Note in particular that for $P_\infty = 0$ an ideal-gas law is recovered.

In this thesis, phase transitions will not be considered. So, the SG-EOS equation (3.1) is generalized as below by considering $e^* = 0$,

$$P = (\gamma - 1)\rho e - \gamma P_\infty \tag{3.2}$$

The stiffened gas equation of state can describe the metastable phase of liquids and gases under high pressure and temperature conditions, such as in shock waves, detonations, or rapid expansions. The metastable phase is a state where the system is not in thermodynamic equilibrium but remains stable for a finite time. The stiffened gas equation of state can account for the effects of repulsion and attraction between molecules, which influence the system's pressure, volume, and energy. For a given fluid, the stiffened-gas equation of state is fully defined by the Helmholtz free energy [67].

Below is a brief review of some properties of the stiffened-gas equation of state considered in this thesis [68].

Thermodynamic properties

Pressure: $$p = (\gamma - 1)\rho e - \gamma p_\infty \tag{3.3}$$

Entropy: $$S(\rho, T) = C_V T \ln\left(\frac{T}{T_0}\left(\frac{\rho_0}{\rho}\right)^{\gamma-1}\right) + S_0 \tag{3.4}$$

Speed of Sound: $$C^2 = \gamma \frac{p + p_\infty}{\rho} \tag{3.5}$$

Ratio of Specific Heats: $$\gamma = \frac{C_p}{C_V} \tag{3.6}$$

Helmholtz Free Energy: $$f(\rho,T) = C_V T\left(1 - \ln\left(\frac{T}{T_0}\right) + (\gamma - 1)\ln\left(\frac{\rho}{\rho_0}\right)\right) - s_0 T + \frac{p_\infty}{\rho} + e_* \quad (3.7)$$

Specific Enthalpy: $$h = e + \frac{p}{\rho} \quad (3.8)$$

Specific Internal Energy: $$e = \frac{p + \gamma p_\infty}{\rho(\gamma - 1)} \quad (3.9)$$

Physical considerations. note that the various parameters of the stiffened-gas equation of state cannot be chosen freely if physically correct thermodynamic behavior is to be reproduced. Throughout this paper, it is consistently assumed that the parameters satisfy the following standard restrictions, which follow from thermodynamic stability theory. for the stiffened-gas equation of state to be physically valid.

$$\gamma > 1 \quad (3.10)$$

$$c_V > 0 \quad (3.11)$$

From the equations 3.3 and 3.5, the below equation for Ratio of Specific Heats, γ and infinite pressure, p_∞ has been derived respectively as below,

$$\gamma = \frac{C^2\rho}{p + p_\infty} \quad (3.12)$$

$$p_\infty = \frac{C^2\rho}{\gamma} - p \quad (3.13)$$

For this thesis, the suitable value for γ and p_∞ need to be calculated. So, from the equation 3.3, 3.8 and 3.13 another simple equation for γ has been derived.

$$\gamma = 1 + \frac{C^2}{h} \quad (3.14)$$

Where, C is velocity (m/s) of sound and h is specific enthalpy (J/Kg). This $\frac{C^2}{h}$ term is dimensionless which comply physically. The equation also expresses that the value of γ will be always more than 1.

3.3 Rapid Expansion

The state calculation has been done by allowing the PLG to expand isentropically from its saturation state. To expand isentropically from the saturation state means to undergo a reversible process in which the entropy remains constant and the fluid changes from a saturated liquid-vapor mixture to a superheated vapor.

In this thesis, PLG is considered CO_2 gas. In the first case, the Pressurized Liquefied CO_2 has been depressurized from its saturation state pressure (5.7 MPa) at 293K temperature to 4.0Mpa step by step where the PLG expands isentropically.

In the second case, the pressure has been increased from its saturation state to different higher pressure. In both cases, the thermodynamics state variables have been recorded by using the Matlab code from the Github Thermodynamics tool for H_2O, H_2, and CO_2 [65]. The code that is used to find out the state variable value is given in the appendix.

The state change data has been used to evaluate SG-EOS and find out suitable values for γ and p_∞ by using the equations 3.12 and 3.13.

In another case, some data has been taken by increasing the temperature from 293K to 403K.

3.4 Data-Driven Process

By using the below Matlab code, the respective state variable data has been taken for the saturation temperature of CO_2.

```
th=thermo('CO2');
T0=293;
[ps,vl,vv]=th.saturation(T0);
th.Tvcalc(T0,vl); % calculates all states at T0 and saturated liquid
s0=th.s;
```

Isentropic Expansion from saturation pressure to lower/higher given pressure P_1.

```
>> % calculate an isentropic expansion to p1
p1=4.50E+06;
s0=5.219907711193639e+04;
th.pscalc(p1,s0);
```

3.5 Density Estimation

The Density Estimation CO_2 for this thesis study has been done separately for the specific set of temperatures and pressure. At the time of state calculation, the Matlab provided the critical density value which is almost same for the all pressure that why it was required to estimate density for different pressure and temperature. The density for the calculation of SG-EOS has been taken by entering the below Matlab code in the thermo Matlab.

```
%Calculation of CO2 Density
>> th = thermo('CO2');
th.Tpcalc(T,P) % T = Temperature and P = Pressure
Rho = th.Mw/th.v  %kg/m3
```

4 Result and Discussion

This section includes thermodynamics state variable data calculation and a graphical representation at the isentropic expansion of pressurized CO_2 from its saturation state at the time of depressurization by using SG-EOS. Where saturation temperature is considered 293k and pressure has been found to be 5.71Mpa. All data has been calculated by using the SG-EOS. The curve fitting has been shown and discussed for the SG-EOS constant ρ, γ and P_∞ in isentropic expansion process.

4.1 Thermodynamics Variable Calculation at Saturation

This thesis study is all about the pressurized liquid CO_2. Carbon dioxide does not have a boiling point at atmospheric pressure as there is no liquid phase of CO_2 at Normal temperature and pressure. It sublimates directly from solid to gas at 194.5K. It can only exist as a liquid at pressures above 520Kpa and temperatures between 216.4K and 304.10K[69]. So, it is predicted in this study for pressurized liquid CO_2 is in saturation point at 293K. Some relevant variables values are represented in Table 4.1 that are needed for further calculations.

Table 4.1: Thermodynamics Variables with Value at Saturation Temperature 293k and Pressure 5.71Mpa.

Sl. No.	Thermodynamics Variables	Symbol	Value	Unit
1	Molecular Weight	Mw	44.0098	g
2	Saturation Pressure	P_s	5.7095e+06	Pa
3	Entropy	S	5.2199e+04	J/K
4	Specific Molar Enthalpy	h	1.1238×10^{07}	J/Kmol
5	Specific Molar Enthalpy	h	2.5541×10^{05}	J/Kmol
6	Sound Velocity	C	339.10	m/s
7	Density	ρ	193.11	Kg/m^3

4.2 Density Estimation

The density of liquid carbon dioxide depends on the temperature and pressure. At standard temperature and pressure (STP), CO_2 is a gas with a density of 1.87 kg/m³. In this thesis study, the density of CO_2 is found to be 1.8161 kg/m³ at temperature (293K) and atmospheric pressure (0.1Mpa). As this thesis aims to rapidly depressurize without changing the temperature, the density value needs to be estimated differently from the Matlab thermo code for different pressure at previously considered saturation temperature 293K. Some of the calculated density values by decreasing and increasing pressure at saturation temperature is given in table 4.2 for further calculation.

Table 4.2: Some Sets of density value calculated in different pressure at the saturation temperature 293K of CO_2.

Sl. No.	Depressurization Process		Pressurization Process	
	Pressure, P(Mpa)	Density, Kg/m^3	Pressure, P(Mpa)	Density, Kg/m^3
1	5.71	193.11	5.71	193.06
2	5.65	186.93	5.80	664.82
3	5.60	182.18	5.90	282.18
4	5.55	177.74	6.10	659.23
5	5.50	173.58	6.30	793.44
6	4.00	97.63	6.40	486.10

The density of CO_2 also calculated at different temperatures and pressure as well that's represented in table 4.3.

Table 4.3: Density in different Pressure and Temperature of CO_2 .

Sl. No.	Temperature, T(K)	Pressure, P(Mpa)	Density,
1	293	4.00	97.63
2	294	4.00	96.74
3	295	4.50	114.50
4	297	5	133.20
5	300	5	128.40
6	301	5	126.94
7	303	5	124.21
8	304	5	122.93

4.2.1 Effect of Pressure on the Density of Carbon Dioxide

The density of carbon dioxide is affected by both temperature and pressure. At standard temperature and pressure (STP), CO_2 is a gas with a density of 1.87 kg/m³. However, as the temperature increases or the pressure decreases, the density of CO_2 decreases. For example, at 293k and 5.71Mpa, the density of CO_2 is 193.11 kg/m^3. On the other hand, as the pressure decreases, the density of CO_2 decreases. For example, at 293k and 4.00Mpa, the density of CO_2 is 97.63 kg/m^3.

4.3 Thermodynamics Values Calculation of CO_2 for Isentropic Expansion Process

The Pressurized Liquid CO_2 has been depressurized from its saturation state where the process is isentropic expansion. In this study, for the sake of SG-EOS value calculation, the thermodynamics state variables value of CO_2 has been calculated from Matlab for isentropic expansion by decreasing the pressure from its saturation state to 4.0 Mpa.

4.3.1 Depressurization (Isentropic Expansion)

In this thesis study, the Pressurized Liquid CO_2 is allowed to be depressurized from the saturation pressure 5.71Mpa to 4.0Mpa at 293k in small interval pressure. A total of 25 sets of data have been calculated the by the process described in methodology (3.4). It was not possible to calculate data after pressure 4.0Mpa. So, this is the last limit to describe the phase transition of pressurized liquid CO_2 in this report. The table 4.4 represents the one set of relevant thermodynamics variables value at depressurization from saturation pressure 5.71Mpa to 4.0Mpa that are used for further calculation.

Table 4.4: Sets of Thermodynamics Variables calculated in Isentropic Expansion process from saturation pressure 5.71Mpa to 4.0Mpa at 293k.

Sl. No.	Thermodynamics Variables	Symbol	Value	Unit
1	Molecular Weight	Mw	44.0098	g
2	Saturation Pressure	p_s	5.71×10^{06}	Pa
3	Pressure Drop	p	4.00×10^{06}	Pa
4	Entropy	S	5.2199×10^{04}	J/K
5	Specific Molar Enthalpy	h	1.1140×10^{07}	J/Kmol
6	Specific Enthalpy	h	2.5318×10^{05}	J/Kg
7	Sound Velocity	C	256.84	m/s
8	Density	ρ	97.63	Kg/m^3

4.3.2 Pressurization (Isentropic Compression)

Isentropic Compression of liquid CO_2, or carbon dioxide, involves increasing the pressure applied to the liquid state of this compound. Carbon dioxide is typically stored and transported in its liquid form under high pressure, which keeps it in a dense and easily manageable state. The pressure of liquid CO_2 has been increased from the saturation pressure 5.71Mpa to

10.0Mpa step by step at 293K. Here, the process is considered as isentropic compression. As in the higher pressure before critical temperature the CO_2 can remain in liquid state. So, no phase transition has occurred in this process. A total of 42 sets of data have been calculated the by the process described in methodology (3.4) from saturation state. The table 4.5 represents the one set of relevant thermodynamics variables value at pressurization from saturation pressure 5.71Mpa to 10.00Mpa that are used for further calculation.

Table 4.5: Sets of Thermodynamics Variables calculated at Isentropic compression Process from saturation pressure 5.71Mpa to 10.0Mpa at 293k.

Sl. No	Thermodynamics Variables	Symbol	Value	Unit
1	Molecular Weight	Mw	44.0098	g
2	Saturation Pressure	p_s	5.71×10^{06}	Pa
3	Pressure up	p	10.00×10^{06}	Pa
4	Entropy	S	5.2199×10^{04}	J/K
5	Specific Molar Enthalpy	h	1.1177×10^{07}	J/Kmol
6	Specific Enthalpy	h	2.6083×10^{05}	J/Kg
7	Sound Velocity	C	417.52	m/s
8	Density	ρ	857.40	Kg/m^3

4.3.3 Depressurization in Isentropic Expansion Process from Different Saturation Temperatures

The temperature of pressurized liquid CO_2 has been increased from the saturation temperature 293K to 304K and allow to expand from corresponding saturation pressure. It is not possible to calculate the thermodynamic properties of CO_2 at more than 304K from the present Matlab thermo code in Github since the critical temperature of CO_2 is 304.10K. Table 4.6 represents the one set of relevant thermodynamics variables value at 300K that are used for further calculation.

Table 4.6: Sets of Thermodynamics Variables calculated at depressurization in Isentropic Expansion process from saturation pressure 7.3Mpa to 5.0Mpa at 303k.

Sl. No.	Thermodynamics Variables	Symbol	Value	Unit
1	Molecular Weight	Mw	44.0098	g
2	Saturation Pressure	p_s	7.36×10^{06}	Pa
3	Pressure drops	p	5.00×10^{06}	Pa
4	Entropy	S	6.1019×10^{04}	J/K
5	Specific Molar Enthalpy	h	1.3759×10^{07}	J/Kmol
6	Specific Enthalpy	h	3.1271×10^{05}	J/Kg
7	Sound Velocity	C	136.35	m/s
8	Density	ρ	122.93	Kg/m^3

4.4 The suitable Value Calculation for SG-EOS Constant (Isentropic Expansion Process)

The SG-EOS stands for the stiffened gas equation of state, which is a simple model that can describe the thermodynamic behavior of liquids and gases under high pressure and temperature conditions. It can be used to model liquids such as water, explosives, CO_2, and PLG etc. The simplest form of SG-EOS is like below which has been used for calculation of the state properties.

$$P = (\gamma - 1)\rho e - \gamma P_\infty \quad 4.1$$

Here γ, ρ and P_∞ is constant which are calculated for curve fitting and the specific internal energy e has been calculated form this equation as well for Isentropic Expansion and compression Process as well as different increasing temperatures. Here one set of calculations has been shown for the isentropic expansion process from saturation state to 4.00Mpa.

4.4.1 Ratio of Specific Heats, γ

It is also known as the heat capacity ratio or the adiabatic index, is the ratio of the heat capacity at constant pressure (C_P) to heat capacity at constant volume (C_V). This is an isentropic expansion factor. The value of γ has been calculated by using the equation (3.14). A sample of calculation of depressurization process from the saturation pressure 5.71Mpa to 4.0Mpa at 293k is given below. The corresponding values for c and h is taken from the table 4.4.

$$\gamma = 1 + \frac{c^2}{h} = 1 + \frac{256.84^2}{2.5318\times10^{05}} = 1.2605$$

4.4.2 Density, ρ

A substance's density can be defined as its mass in relation to its unit volume. The density of a substance can changes in response to changes in temperature, pressure, and the chemical make-up of the substance. Because density is an intense attribute, its value does not change regardless of the quantity of the substance being considered. The density of CO_2 at 4.0Mpa pressure and 293k temperature is taken from the table 4.2 which has been estimated as per sub section 3.5 of methodology.

ρ = 97.6268 Kg/m^3

4.4.3 Pressure Infinite, P_∞

P∞ is the infinite pressure, which is the pressure that the substance would have if it were compressed to zero volume. It is a measure of the attractive forces between the molecules of the substance. Sometimes it is also called pressure correction as it represents the cohesion pressure. The value of this constant has been calculated using the equation (3.13) at depressurization from the saturation pressure 5.71Mpa to 4.0Mpa at 293k is given below. The corresponding values for c and p is taken from the table 4.4. and p value is taken from the table 4.2 whereas the γ has taken from the previous section.

$$p_\infty = \frac{C^2\rho}{\gamma} - p$$

$$\Rightarrow \quad p_\infty = \frac{256.8441^2\times97.6268}{1.2605} - 4.0\times10^6 \text{ pa} \quad => \; p_\infty = 1.1091\times10^6 \text{pa}$$

4.4.4 Specific Internal Energy, e

The amount of energy that is stored in the internal structure of a substance, such as the molecular bonds and motion of its constituent molecules, is referred to as the specific internal energy of the substance. It is a thermodynamics parameter t in thermodynamics and important to understand the energy content of materials and their changes during various processes. The Specific Internal Energy, e of CO_2 at isentropic expansion process from the saturation pressure 5.71Mpa to 4.0Mpa at 293k is calculated by the equation (3.9). The corresponding values for p and ρ are taken respectively from the table 4.4. and table 4.2 whereas values γ and p_∞ are taken from the subsection 4.3.1 and 4.3.3. respectively.

$$e = \frac{p+\gamma p_\infty}{\rho(\gamma-1)}$$

$$e = \frac{4.0\times10^6+ 1.2605\times1.1091\times10^6}{97.6268\times(1.2605-1)}$$

$$e = 2.1220 \times 10^{05}\ J/Kg$$

The similar calculation has been applied for the pressurization and different temperatures data calculations to find out γ, ρ, P_∞ and e for SG-EOS. All the calculated data has been shown in table 4.7, 4.8 and 4.9 which are used further for curve fitting of SG-EOS constants.

Table 4.7: All Calculated Data Set for Isentropic Expansion at Saturation Temperature 293K of CO_2 from 5.71 Mpa to 4.0Mpa, Entropy is 5.22×104 J/K.

Sl. No.	Pressure, P(Mpa)	Density, ρ (kg/m3) @ (T, P)	Sound Velocity, C (m/s)	Specific Enthalpy, h (J/kg) × 10^{05}	Ratio of Specific Heat, γ	Infinity Pressure, P∞ (MPa)	Specific Internal energy, e (j/kg) × 10^{05}
1	5.71	193.11	339.10	2.5541	1.4502	9.6025	2.2584
2	5.65	186.93	337.51	2.5533	1.4461	9.0747	2.2511
3	5.60	182.18	336.15	2.5527	1.4426	8.6692	2.2453
4	5.55	177.74	334.77	2.5520	1.4391	8.2914	2.2398
5	5.50	173.58	333.36	2.5514	1.4355	7.9369	2.2345
6	5.45	169.65	331.92	2.5507	1.4319	7.6024	2.2295
7	5.40	165.91	330.45	2.5501	1.4282	7.2850	2.2246
8	5.35	162.35	328.94	2.5494	1.4244	6.9827	2.2199
9	5.30	158.94	327.41	2.5488	1.4205	6.6938	2.2153
10	5.25	155.67	325.83	2.5481	1.4166	6.4167	2.2109
11	5.20	152.53	324.22	2.5475	1.4126	6.1502	2.2066
12	5.15	149.50	322.56	2.5468	1.4085	5.8932	2.2023
13	5.10	146.57	320.86	2.5462	1.4043	5.6448	2.1982
14	5.05	143.73	319.11	2.5455	1.4000	5.4041	2.1942
15	5.00	140.98	317.30	2.5449	1.3956	5.1704	2.1902
16	4.90	135.71	313.52	2.5436	1.3864	4.7215	2.1825
17	4.80	130.72	309.46	2.5423	1.3767	4.2931	2.1751
18	4.70	125.97	305.07	2.5410	1.3662	3.8812	2.1679
19	4.60	121.43	300.31	2.5397	1.3551	3.4817	2.1608
20	4.50	117.09	295.07	2.5383	1.3430	3.0910	2.1540
21	4.40	112.91	289.27	2.5370	1.3298	2.7051	2.1473
22	4.30	108.89	282.77	2.5357	1.3153	2.3196	2.1408
23	4.20	105.01	275.38	2.5344	1.2992	1.9296	2.1344
24	4.10	101.26	266.86	2.5331	1.2811	1.5289	2.1282
25	4.00	97.63	256.84	2.5318	1.2605	1.1091	2.1220

Table 4.8: All Calculated Data Set for Isentropic Compression Process at Saturation Temperature 293K of CO_2 from 5.71 Mpa to 10.0Mpa, Entropy is 5.22×10^4 J/K.

Sl. No.	Pressure, P(Mpa)	Density, ρ (kg/m3) @ (T, P)	Sound Velocity, C (m/s)	Specific Enthalpy, h (J/kg) $\times 10^{05}$	Ratio of Specific Heat, γ	Infinity Pressure, P∞ (MPa)	Specific Internal energy, e (j/kg) $\times 10^{05}$
1	5.71	193.06	339.10	2.5541	1.4502	9.60	2.2584
2	5.80	664.82	341.45	2.5552	1.4563	47.43	2.4680
3	5.90	282.18	343.98	2.5565	1.4628	16.92	2.3474
4	6.10	659.23	348.83	2.5591	1.4755	48.26	2.4666
5	6.30	793.44	353.43	2.5617	1.4876	60.32	2.4823
6	6.40	486.10	355.66	2.5630	1.4935	34.77	2.4313
7	6.50	486.10	357.84	2.5642	1.4994	35.01	2.4305
8	6.60	486.50	359.98	2.5655	1.5051	35.29	2.4298
9	6.70	486.91	362.07	2.5668	1.5107	35.55	2.4292
10	6.80	648.93	364.13	2.5681	1.5163	49.95	2.4633
11	6.90	647.66	366.16	2.5693	1.5218	50.16	2.4628
12	7.00	810.22	368.15	2.5706	1.5272	64.90	2.4842
13	7.10	812.33	370.11	2.5719	1.5326	65.50	2.4845
14	7.20	814.38	372.04	2.5732	1.5379	66.10	2.4847
15	7.30	816.38	373.94	2.5744	1.5432	66.68	2.4850
16	7.40	818.32	375.82	2.5757	1.5483	67.25	2.4853
17	7.50	820.22	377.66	2.5770	1.5535	67.81	2.4855
18	7.60	822.07	379.49	2.5782	1.5586	68.36	2.4858
19	7.70	823.88	381.29	2.5795	1.5636	68.90	2.4860
20	7.80	825.65	383.06	2.5808	1.5686	69.44	2.4863
21	7.90	827.39	384.82	2.5820	1.5735	69.97	2.4866
22	8.00	829.08	386.55	2.5833	1.5784	70.48	2.4868
23	8.10	830.74	388.26	2.5846	1.5833	71.00	2.4871
24	8.20	832.37	389.95	2.5858	1.5881	71.50	2.4873
25	8.30	632.92	391.62	2.5871	1.5928	52.64	2.4559

Sl. No.	Pressure, P(Mpa)	Density, ρ (kg/m3) @ (T, P)	Sound Velocity, C (m/s)	Specific Enthalpy, h (J/kg) × 1005	Ratio of Specific Heat, γ	Infinity Pressure, P∞ (MPa)	Specific Internal energy, e (j/kg) × 1005
26	8.40	835.54	393.27	2.5883	1.5975	72.49	2.4878
27	8.50	494.11	394.91	2.5896	1.6022	39.59	2.4176
28	8.60	494.51	396.52	2.5909	1.6069	39.79	2.4169
29	8.70	840.07	398.12	2.5921	1.6115	73.93	2.4885
30	8.80	628.53	399.70	2.5934	1.6160	53.34	2.4534
31	8.90	627.69	401.27	2.5946	1.6206	53.47	2.4528
32	9.00	844.38	402.82	2.5959	1.6251	75.31	2.4893
33	9.10	845.77	404.35	2.5971	1.6296	75.76	2.4895
34	9.20	847.14	405.87	2.5984	1.6340	76.21	2.4898
35	9.30	848.49	407.38	2.5996	1.6384	76.65	2.4900
36	9.40	849.82	408.87	2.6009	1.6428	77.08	2.4903
37	9.50	851.13	410.34	2.6021	1.6471	77.51	2.4905
38	9.60	852.42	411.80	2.6034	1.6514	77.93	2.4907
39	9.70	853.69	413.25	2.6046	1.6557	78.36	2.4910
40	9.80	854.94	414.69	2.6059	1.6599	78.77	2.4912
41	9.90	856.18	416.11	2.6071	1.6641	79.18	2.4915
42	10.00	857.40	417.52	2.6083	1.6683	79.59	2.4917

Table 4.9: All Calculated Data Set for Isentropic Expansion at different Saturation Temperature and pressure of CO_2

Sl. No.	Pressure, P(Mpa)	Density, ρ (kg/m3) @ (T, P)	Sound Velocity, C (m/s)	Specific Enthalpy, h (J/kg) × 10^{05}	Ratio of Specific Heat, γ	Infinity Pressure, P∞ (Pa)	Specific Internal energy, e (j/kg) × 10^{05}
1	4.00	97.63	256.85	2.53176	1.26058	1.1E+06	2.1220
2	4.00	96.74	191.36	2.56406	1.14282	-9.0E+05	2.1506
3	4.50	114.50	221.20	2.60435	1.18787	2.2E+05	2.2113

4	5.00	133.20	157.65	2.68301	1.09263	-2.0E+06	2.3076
5	5.00	128.40	138.36	2.79619	1.06846	-2.7E+06	2.4068
6	5.00	126.94	137.18	2.84676	1.06611	-2.8E+06	2.4529
7	5.00	124.21	135.63	2.98137	1.06171	-2.8E+06	2.5788
8	5.00	122.93	136.35	3.12711	1.05945	-2.8E+06	2.7204

4.5 Curve Fitting (Isentropic Expansion Process)

On the consideration of all calculated data above for sake of this thesis study the below curve fitting has been done for P_∞ and γ to evaluate that it could be possible to use the stiffened gas EOS to calculate states along a constant entropy process. In this thesis study, isentropic expansion process has been used from saturation state (293K) to 4.0Mpa to fit the curve. Though isentropic compression data has been calculated, those data are not suitable for curve fitting.

4.5.1 Pressure Vs Density of CO_2

The figure 4.1 and 4.2 shows the density of CO_2 in two process at 293K where at the time of depressurization the density has been decreased linearly which is regular phenomenon. On the other hand, in the pressurization process, the density curve is looks like unstable to predict. It can be said in the high pressure at 8Mpa the density curve looks stable and increasing continuously.

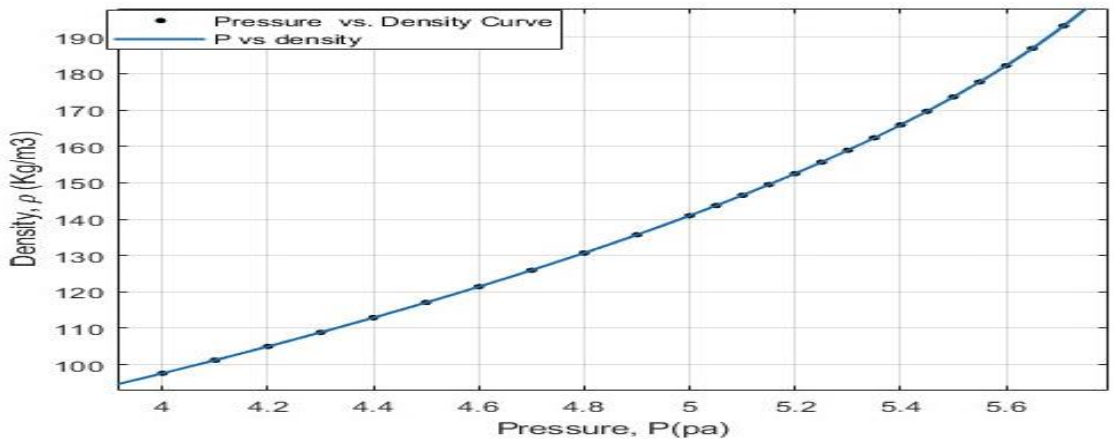

Figure 4.1: Pressure vs Density of CO_2 in term of rapid depressurization from 5.71 to 4 Mpa at 293k in isentropic expansion process.

4.5.2 Pressure Vs Ratio of Specific Heat Curve

The "Pressure vs. Ratio of Specific Heat" CO_2 reveals valuable insights into how this gas behaves under different thermodynamic conditions. CO_2 is a real gas, and its behavior is more complex than that of an ideal gas due to intermolecular forces and other factors. As a result, its ratio of specific heat (γ) can vary with pressure and temperature. In this thesis study, the behavior of γ has been modelled in the isentropic expansion process by decreasing and increasing the pressure using SG-EOS. The figure 4.2 shows the depressurization in the isentropic expansion process.

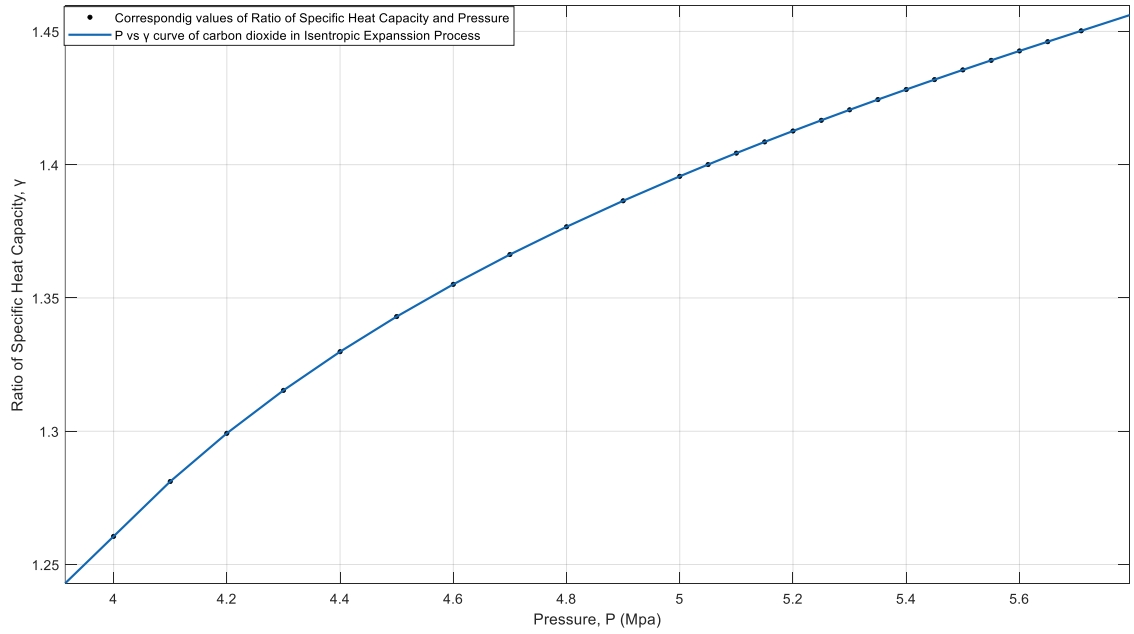

Figure 4.2: Pressure Vs Ratio of Specific Heat Curve of CO_2 in rapid depressurization from 5.71 to 4 Mpa at 293k in isentropic expansion process.

In the depressurization process the γ decreases with pressure linearly and vice versa for higher pressure. That means that γ might decrease significantly at depressurization from any pressure point which indicates higher compressibility that means the phase might have trends to transit from liquid to gas. γ might experience a noticeable rise due to increased molecular interactions and density effects. CO_2 might show possible phase transitions to denser states. The isentropic process can be describe using SG-EOS.

4.5.3 Pressure Vs Pressure Infinite Curve

The figure 4.3 shows the relationship between the actual pressure P and pressure Infinite P_∞ for CO_2 in isentropic expansion process that has been modeled by stiffened gas equation of state. The infinity pressure P_∞ is a parameter that represents the limit of the pressure as the volume approaches zero.

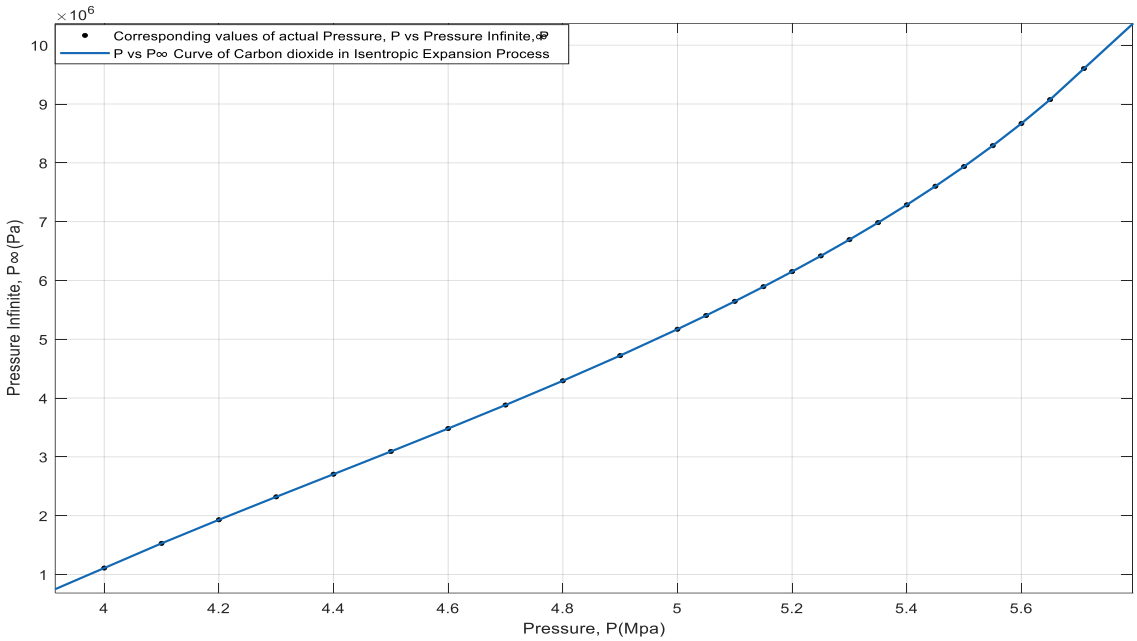

Figure 4.3: Pressure vs Pressure infinite curve in depressurization at 293K from 5.71 to 4 Mpa in isentropic expansion process.

4.5.4 Pressure Infinite Vs Ratio of Specific Heat Curve

The figure 4.4 shows the relationship between the pressure Infinite P_∞ and the ratio of specific heat γ for a fluid that can be modeled by a stiffened gas equation of state. The infinity pressure P_∞ is a parameter that represents the limit of the pressure as the volume approaches zero. The ratio of specific heat γ is a measure of the compressibility of the fluid and the amount of heat transferred during an adiabatic process.

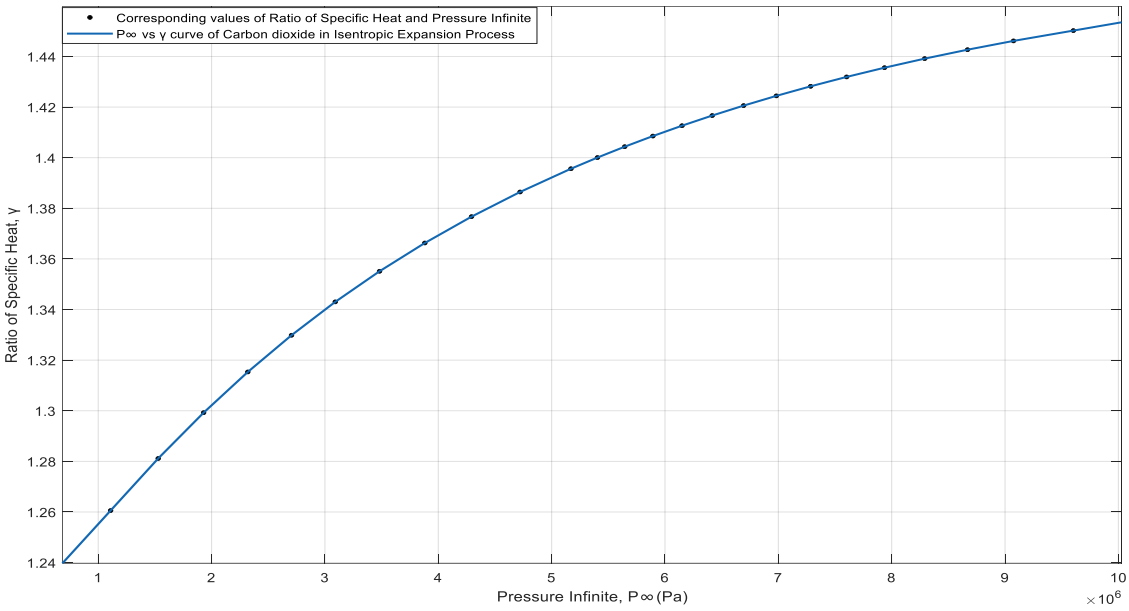

Figure 4.4: Pressure Infinite vs Ratio of Specific Heat curve of CO_2 in depressurization at 293K from 5.71 to 4 Mpa in isentropic expansion process.

The figure 4.4 shows that the infinity pressure P_∞ and the ratio of specific heat γ are nonlinearly related, with a convex shape. The blue line is a smooth curve that increases from left to right. This means that as the infinity pressure P_∞ decreases, the ratio of specific heat γ also decreases, but at an increasing rate. The shape of the curve indicates that there is a trade-off between the pressure Infinite and the heat capacity ratio of the CO_2 in the depressurization process.

The figure also shows that the infinity pressure P_∞ and the ratio of specific heat γ have different units and orders of magnitude. The infinity pressure P_∞ is measured in pascals (Pa), which are units of force per unit area. The ratio of specific heat γ is dimensionless, which means it has no units. The infinity pressure P_∞ ranges from 1 to 10 MPa, which are very small

values compared to typical pressures in fluids. The ratio of specific heat γ ranges from 1.28 to 1.44, which is close to the values for ideal gases (around 1.33).

4.5.5 Pressure Vs Specific Energy Curve

The figure 4.5 shows the relationship between pressure and specific internal energy modelled by SG-EOS. The graph is a scatter plot with a blue line connecting the points. The line has a positive slope and appears to be linear. In the rapid depressurization with isentropic process the modelled curve shows proper thermodynamics behaviour of CO_2 where internal energy of matter is reducing with pressure decrease and going closer to phase change. This relationship is linear, meaning that for every unit increase in pressure, there is a constant increase in specific internal energy.

The x-axis ranges from 4.0 to 5.6 MPa and the y-axis ranges from 2.12 to 2.26 x 10^5 J/kg. There is no sharp change of the curve since it can be said that the phase transition rate would be smaller.

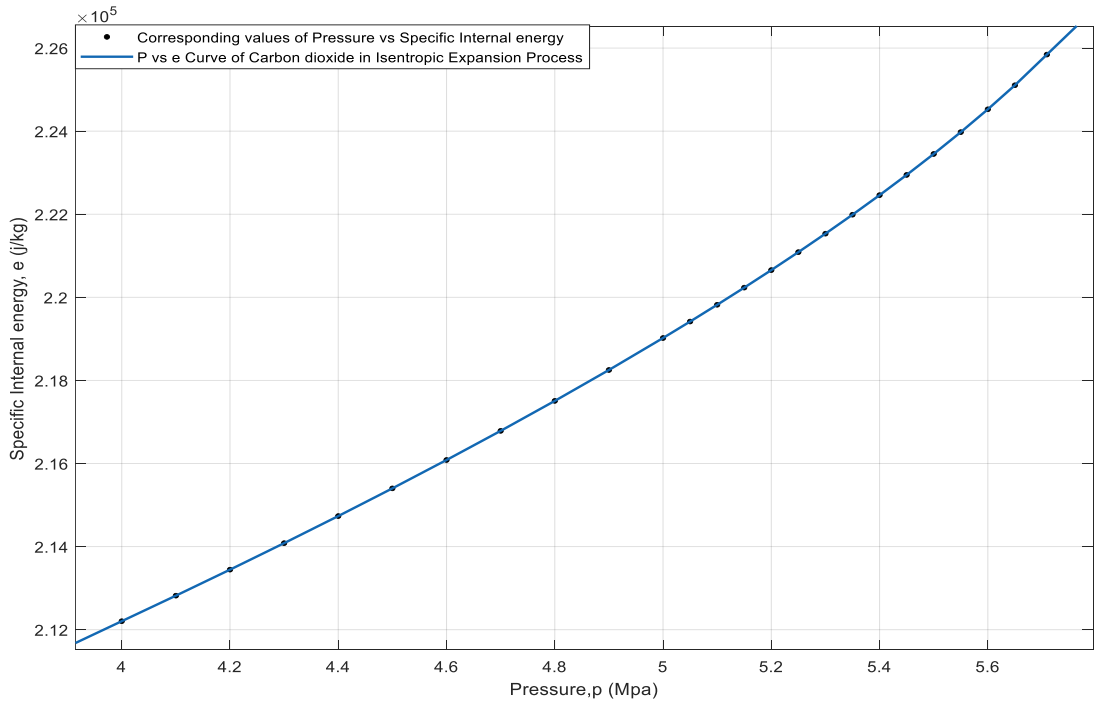

Figure 4.5: Pressure vs Specific Internal Energy curve in depressurization at 293K from 5.71 to 4 Mpa in isentropic expansion process.

4.6 Overall Discussion

The physical significance of the figure p_∞ vs γ is:

- It shows how the stiffened pressure infinite, and the heat capacity of a fluid are related by the stiffened gas equation of state.
- It can be used to estimate the value of γ for a given value of P_∞, or vice versa.
- It can be used to compare different fluids or phases based on their P_∞ and γ values.

All the curve above has been made to calculate thermodynamics states of CO_2 along a constant entropy expansion process from the saturation state(293K). In this section, the SG-EOS has been evaluated by taking value from the above curve fitting for a specific pressure, p = 4.75Mpa. The corresponding values of SG-EOS is given below which are taken from above curves for pressure p = 4.75Mpa.

Table 4.10: SG-EOS parameters values from curves fitting for isentropic expansion process.

Parameters	Source
Ratio of Specific Heat, $\gamma = 1.37$	Figure 4.3
Pressure Infinite, $P_\infty = 4.09$Mpa	Figure 4.4
Specific Internal Energy, $e = 2.17\times10^5$ J/Kg	Figure 4.6
Density, $\rho = 128.3881$Kg/m^3	From Matlab for 293K and 4.75Mpa

The SG-EOS:

$$P = (\gamma - 1)\rho e - \gamma P_\infty$$

$$P = (1.37 - 1) \times\ 128.3881 \times 2.17 \times 10^5 - 1.37 \times 4.09 \times 10^5$$

$$P = 4.75\text{Mpa}$$

The actual pressure has been calculated by using the data from the curves above which demonstrated that the stiffened gas EOS is well enough to calculate states along a constant entropy expansion process.

For the same pressure P, the value γ and P_∞ in the figure 4.3 and 4.4 fitted in the same point in figure 4.5. So, the P_∞ vs γ curve has best fitted for isentropic expansion process.

5 Conclusion

In the course of this study, a comprehensive exploration of carbon dioxide's (CO_2) behavior during rapid depressurization has been meticulously undertaken. The central focus of the investigation was the isentropic expansion process, shedding light on the intricate interplay between various thermodynamic parameters. This study delved into the intricate behavior of carbon dioxide (CO_2) undergoing rapid depressurization, a phenomenon critical for understanding processes like Boiling Liquid Expanding Vapor Explosions (BLEVEs). The analysis of the relationship between the infinite pressure (P_∞) and the specific heat ratio (γ) was of utmost importance. The outcomes highlighted a non-linear yet fascinating link, symbolized by a convex curve. With regard to CO_2's behavior during depressurization, this relationship, as explained by the Stiffened Gas Equation of State (SG-EOS), has significant ramifications that shed light on phase transitions and potential explosive tendencies. However, the highlight of this study lies in its in-depth analysis of the isentropic expansion process where SG-EOS is used efficiently from saturation state (293K and 5.71Mpa) to 4Mpa. By leveraging the power of the SG-EOS, this investigation provided a detailed evaluation of CO_2's responses within this context. Notably, the study established a direct linear correlation between pressure and specific internal energy, unraveling the underlying dynamics of phase transitions in the face of rapid depressurization. Furthermore, the study explored the role of the stiffened gas equation of state in modeling the behavior of CO_2. The investigation also underscored the suitability of the stiffened gas equation for estimating thermodynamic states along a constant entropy expansion process. In summary, this report advances our understanding of CO_2's behavior in rapid depressurization scenarios, with particular emphasis on the isentropic expansion process. The intricate relationship between pressure infinity ($P\infty$) and the ratio of specific heat (γ) serves as a cornerstone in deciphering CO_2's dynamic responses during such extreme conditions. Through theoretical exploration and empirical insights, this study contributes to the broader comprehension of fluid behavior under rapid depressurization, paving the way for enhanced safety protocols and informed engineering decisions.

5.1 Future Research Recommendation:

The behavior of carbon dioxide (CO_2) during rapid depressurization in isentropic expansion process has been clarified by this work, but there are still a number of directions that need to be explored in order to further our understanding and the range of applications for the results. The suggestions listed below offer potential lines of inquiry for upcoming studies:

1. Temperature Dependency: Investigating how CO_2 behaves under rapid depressurization in different temperature ranges may reveal subtle differences. This requires a deeper comprehension of the equation of state, taking temperature into account as a variable.

2. Validation through Experimentation

While this study primarily employs theoretical models, validating the findings through controlled experimental setups would add a layer of confidence to the conclusions. Experimental data could also facilitate the refinement of existing models.

3. Influence of Impurities

It is worthwhile to investigate how CO_2 behaves under rapid depressurization in the presence of contaminants or other impurities. Impurities may change the dynamics of the phase transition and may have an impact on safety concerns.

3. Multi-Component Systems

Extending the research to include CO_2 and other multi-component systems may shed light on the intricate interactions that take place during rapid depressurization. It could be quite useful to study how various components affect phase transitions and explosive tendencies.

4. Dynamic Scenarios Modelling

Considering dynamic scenarios involving rapid depressurization, such as those encountered in real-world industrial processes, could provide more accurate insights into CO_2's behavior. Simulating scenarios with varying initial conditions and rates of depressurization could yield valuable information.

References

[1] T. Abbasi and S. A. Abbasi, “The boiling liquid expanding vapour explosion (BLEVE) is fifty ... and lives on!,” *J Loss Prev Process Ind*, vol. 21, no. 4, pp. 485–487, Jul. 2008.

[2] A. M. Birk, C. Davison, and M. Cunningham, “Blast overpressures from medium scale BLEVE tests,” *J Loss Prev Process Ind*, vol. 20, no. 3, pp. 194–206, Jul. 2007.

[3] H. T. Kohlbrand, “Critical aspects of safety and loss prevention. Trevor A. Kletz, Butterworths, Stoneham, MA, 1990, 349 pp.,57.95,” *AIChE Journal*, vol. 37, no. 5, p. 800, Jul. 1991.

[4] “What firefighters need to know about BLEVEs.”

[5] R. W. Prugh, “Quantitative Evaluation of ‘Bleve’ Hazards,” *Journal of Fire Protection Engineering*, vol. 3, no. 1, pp. 9–24, Jan. 1991.

[6] the Center for Chemical Process Safety (CCPS), *Guidelines for Vapor Cloud Explosion, Pressure Vessel Burst, BLEVE, and Flash Fire Hazards*, 2nd ed. John Wiley & Sons, 2011.

[7] T. Abbasi and S. A. Abbasi, “Accidental risk of superheated liquids and a framework for predicting the superheat limit,” *J Loss Prev Process Ind*, vol. 20, no. 2, pp. 165–181, Jul. 2007.

[8] D. Bjerketvedt, K. Egeberg, W. Ke, A. Gaathaug, K. Vaagsaether, and S. H. Nilsen, “Boiling liquid expanding vapour explosion in CO_2 small scale experiments,” *Energy Procedia*, vol. 4, pp. 2285–2292, 2011.

[9] W. E. Clayton and M. L. Griffin, “Catastrophic failure of a liquid carbon dioxide storage vessel,” *Process Safety Progress*, vol. 13, no. 4, pp. 202–209, Jul. 1994.

[10] Y. Zhang, J. Schork, and K. Ludwig, “292075 Revisiting the Conditions and Consequences of CO_2 Tank Explosions,” Jul. 2013.

[11] D. R. Olander, *General Thermodynamics*. Boca Raton: CRC, 2008.

[12] D. W. , H. P. G. and A. C. Oxtoby, “Phase Transition,” in *Principles of Modern Chemistry*, 6th ed.Singapore: Thomson/Brooks/Cole, pp. 428–430.

[13] S. Bhuyan, “Carbon Dioxide (CO_2) Phase Diagram.” Feb. 2023.

[14] “Thermal Properties of Materials – Definition,” *https://material-properties.org/thermal-properties-of-materials-definition/?utm_content=cmp-true*, Apr. 10, 2023.

[15] P. V. Skripov and A. P. Skripov, “The phenomenon of superheat of liquids: In memory of Vladimir P. Skripov,” in *International Journal of Thermophysics*, May 2010, pp. 816–830. doi: 10.1007/s10765-010-0738-4.

[16] M. Hansen, *Experimental and theoretical studies of rapid phase transitions in CO 2*. 2018.

[17] Vladimir Pavlovich Skripov, *Metastable Liquids*. New York: Halsted Press, John Wiley & Sons, 1974.

[18] R. C. Reid, *Am. Sci.*, vol. 64. 1976.

[19] B. L. Beegle, M. Modell, and R. C. Reid, "Thermodynamic stability criterion for pure substances and mixtures," *AIChE Journal*, vol. 20, no. 6, pp. 1200–1206, 1974, doi: https://doi.org/10.1002/aic.690200621.

[20] Mengmeng Xie, "Thermodynamic and gasdynamic aspects of a boiling liquid expanding vapour explosion," Thesis Report, Delft University of Technology, The Netherlands, 2013.

[21] P. Spiegler, J. Hopenfeld, M. Silberberg, C. F. Bumpus, and A. Norman, "Onset of stable film boiling and the foam limit," *Int J Heat Mass Transf*, vol. 6, no. 11, pp. 987–989, Apr. 1963.

[22] J. H. Lienhard, "Corresponding States Correlations of the Spinodal and Homogeneous Nucleation Limits," *J Heat Transfer*, vol. 104, no. 2, pp. 379–381, May 1982.

[23] M. Volmer and . Weber, "Keimbildung in übersättigten Gebilden," *Zeitschrift für Physikalische Chemie*, vol. 119U, no. 1, pp. 277–301, Jan. 1926.

[24] M. Blander and J. L. Katz, "Bubble nucleation in liquids," *AIChE Journal*, vol. 21, no. 5, pp. 833–848, Apr. 1975.

[25] R. Cole, "Boiling nucleation," in *Advances in heat transfer*, Elsevier, 1974, pp. 85–166.

[26] V. P. Carey, *Liquid-Vapor Phase-Change Phenomena: An Introduction to the Thermophysics of Vaporization and Condensation in Heat Transfer Equipment*. 1992.

[27] D. W. Oxtoby, "Homogeneous nucleation: theory and experiment," *Journal of Physics: Condensed Matter*, vol. 4, no. 38, pp. 7627–7650, Sep. 1992.

[28] G. S. Bankoff, "Proceedings of the 6th International Heat Transfer Conference," Hemisphere, Toronto, 1978, p. 355.

[29] J. R. SIM\~ OES-MOREIRA and J. E. SHEPHERD, "Evaporation waves in superheated dodecane," *J Fluid Mech*, vol. 382, pp. 63–86, Mar. 1999.

[30] R. SAUREL, F. PETITPAS, and R. ABGRALL, "Modelling phase transition in metastable liquids: application to cavitating and flashing flows," *J Fluid Mech*, vol. 607, pp. 313–350, Jun. 2008.

[31] Wei Ke, "CO_2 BLEVE (Boiling Liquid Expanding Vapor Explosion)," Telemark University College, Porsgrunn, 2009.

[32] R. C. Reid, "Possible Mechanism for Pressurized-Liquid Tank Explosions or BLEVE's," *Science (1979)*, vol. 203, no. 4386, pp. 1263–1265, Mar. 1979.

[33] G. A. Pinhasi, A. Ullmann, and A. Dayan, "1D plane numerical model for boiling liquid expanding vapor explosion (BLEVE)," *Int J Heat Mass Transf*, vol. 50, no. 23–24, pp. 4780–4795, Jul. 2007.

[34] R. W. Prugh, “Quantitative evaluation of fireball hazards,” *Process Safety Progress*, vol. 13, no. 2, pp. 83–91, Jul. 1994.

[35] T. ABBASI and S. ABBASI, “The boiling liquid expanding vapour explosion (BLEVE): Mechanism, consequence assessment, management,” *J Hazard Mater*, vol. 141, no. 3, pp. 489–519, Mar. 2007.

[36] J. M. Salla, M. Demichela, and J. Casal, “BLEVE: A new approach to the superheat limit temperature,” *J Loss Prev Process Ind*, vol. 19, no. 6, pp. 690–700, Jul. 2006.

[37] CCPS, “Guidelines for evaluating the characteristics of vapor cloud explosions, flash fires, and BLEVEs,” New York, NY, 1994.

[38] M. M. van der Voort *et al.*, “An experimental study on the temperature dependence of CO_2 explosive evaporation,” *J Loss Prev Process Ind*, vol. 26, no. 4, pp. 830–838, Jul. 2013.

[39] E. Sher, T. Bar-Kohany, and A. Rashkovan, “Flash-boiling atomization,” *Prog Energy Combust Sci*, vol. 34, no. 4, pp. 417–439, Jul. 2008.

[40] A. Prosperetti and M. S. Plesset, “Vapour-bubble growth in a superheated liquid,” *J Fluid Mech*, vol. 85, no. 02, p. 349, Jul. 1978.

[41] E. M. de Sá, E. Meyer, and V. Soares, “Adiabatic nucleation in the liquid–vapor phase transition,” *J Chem Phys*, vol. 114, no. 19, pp. 8505–8510, May 2001.

[42] C. F. Delale, J. Hruby, and F. Marsik, “Homogeneous bubble nucleation in liquids: The classical theory revisited,” *J Chem Phys*, vol. 118, no. 2, pp. 792–806, Dec. 2002.

[43] J. E. Shepherd and B. Sturtevant, “Rapid evaporation at the superheat limit,” *J Fluid Mech*, vol. 121, no. 1, p. 379, Jul. 1982.

[44] C. A. McDevitt, C. K. Chan, F. R. Steward, and K. N. Tennankore, “Initiation step of boiling liquid expanding vapour explosions,” *J Hazard Mater*, vol. 25, no. 1–2, pp. 169–180, Jul. 1990.

[45] I. R. M. Leslie and A. M. Birk, “State of the art review of pressure liquefied gas container failure modes and associated projectile hazards,” *J Hazard Mater*, vol. 28, no. 3, pp. 329–365, Jul. 1991.

[46] A. B. H. B. and J. C. M. S. Lesin, “Experimental studies of direct contact boiling at the superheat limit,” *High Temperature*, pp. 866–884, 1993.

[47] J. E. Shepherd and B. Sturtevant, “Rapid evaporation at the superheat limit,” *J Fluid Mech*, vol. 121, no. 1, p. 379, Jul. 1982.

[48] H. Mccann, L. J. Clarke, and A. P. Masters, “An experimental study of vapour growth at the superheat limit temperature,” *Int J Heat Mass Transf*, vol. 32, no. 6, pp. 1077–1093, Jul. 1989.

[49] D. Frost and B. Sturtevant, “Effects of Ambient Pressure on the Instability of a Liquid Boiling Explosively at the Superheat Limit,” *J Heat Transfer*, vol. 108, no. 2, pp. 418–424, May 1986.

[50] D. L. Frost, “Dynamics of explosive boiling of a droplet,” *Physics of Fluids*, vol. 31, no. 9, pp. 2554–2561, Jul. 1988.

[51] G. R. Moore, “Vaporization of superheated drops in liquids,” University of Wisconsin, Madison, Wisconsin, 1956.

[52] V. T. Nguyen, R. M. Furzeland, and M. J. M. Ijpelaar, “Rapid evaporation at the superheat limit,” *Int J Heat Mass Transf*, vol. 31, no. 8, pp. 1687–1700, Jul. 1988.

[53] H.-C. Park, K.-T. Byun, and H.-Y. Kwak, “Explosive boiling of liquid droplets at their superheat limits,” *Chem Eng Sci*, vol. 60, no. 7, pp. 1809–1821, Jul. 2005.

[54] “Boiling liquid expanding vapor explosion - Wikipedia.” Jul. 2011.

[55] L. G. Hill, “An experimental study of evaporation waves in a superheated liquid,” California Institute of Technology, California, USA, 1990.

[56] O. M. Ibrahim, P. M. Hansen, D. Bjerketvedt, and K. Vågsæther, “Evaporation characteristics during decompression of liquified CO_2 from a conical-shaped vessel,” *Results in Engineering*, vol. 12, Dec. 2021, doi: 10.1016/j.rineng.2021.100304.

[57] P. K. Das, G. S. Bhat, and V. H. Arakeri, “Investigations on the propagation of free surface boiling in a vertical superheated liquid column,” *Int J Heat Mass Transf*, vol. 30, no. 4, pp. 631–638, Jul. 1987.

[58] E. Hahne and G. Barthau, “Evaporation waves in flashing processes,” *International Journal of Multiphase Flow*, vol. 26, no. 4, pp. 531–547, Jul. 2000.

[59] P. Reinke and G. Yadigaroglu, “Explosive vaporization of superheated liquids by boiling fronts,” *International Journal of Multiphase Flow*, vol. 27, no. 9, pp. 1487–1516, Jul. 2001.

[60] G. Ciccarelli, J. Melguizo-Gavilanes, and J. Shepherd, “Pressure Field Produced by the Rapid Vaporization of a CO_2 Liquid Column,” 2017, pp. 1293–1297. doi: 10.1007/978-3-319-44866-4_87.

[61] Sindre Tøsse, “The rapid depressurization and evaporation of liquified carbon dioxide,” University College of Southeast Norway, Porsgrunn, Norway, 2017.

[62] E. Hahne and G. Barthau, “Evaporation waves in flashing processes,” *International Journal of Multiphase Flow*, vol. 26, no. 4, pp. 531–547, Jul. 2000.

[63] M. M. van der Voort, A. C. van den Berg, D. J. E. M. Roekaerts, M. Xie, and P. C. J. de Bruijn, “Blast from explosive evaporation of carbon dioxide: experiment, modeling and physics,” *Shock Waves*, vol. 22, no. 2, pp. 129–140, Feb. 2012.

[64] K. B. Mishra, K.-D. Wehrstedt, and H. Krebs, “Boiling Liquid Expanding Vapour Explosion (BLEVE) of Peroxy-fuels: Experiments and Computational Fluid Dynamics (CFD) Simulation,” *Energy Procedia*, vol. 66, pp. 149–152, 2015.

[65] are-mj, “GitHub - are-mj/thermodynamics: Thermodynamics tool for H2O, H2, and CO_2.” May 2023.

[66] “Properties from Helmholtz.”

[67] R. Menikoff, “Empirical Equations of State for Solids,” in *ShockWave Science and Technology Reference Library*, Y. Horie, Ed., Berlin, Heidelberg: Springer Berlin Heidelberg, 2007, pp. 143–188. doi: 10.1007/978-3-540-68408-4_4.

[68] T. Flatten, A. Morin, and S. T. Munkejord, “On solutions to equilibrium problems for systems of stiffened gases,” *SIAM J Appl Math*, vol. 71, no. 1, pp. 41–67, 2011, doi: 10.1137/100784321.

[69] “Liquid carbon dioxide - Wikipedia.” May 2019.

Appendices

Appendix A : Thesis Title, Task Background and Description.

University of South-Eastern Norway

Faculty of Technology, Natural Sciences and Maritime Sciences, Campus Porsgrunn

FMH606 Master's Thesis

Title: Phase transition in rapid depressurization of liquefied gases

USN supervisor: Knut Vågsæther

External partner: Possibly IRSN

Task background:
When liquefied gasses, stored, or transported at saturation pressures above atmosphericpressures, undergo a depressurization the phase transition can act like an explosion. Thisfast phase transition leading to blast waves are usually called BLEVEs (Boiling Liquid Expanding Vapor Explosions). During the depressurization the liquid is expanded into a metastable state before the homogeneous nucleation starts. USN has worked on this phenomena for many years and produced experimental data and started modelling.The rapid phase transition of pressurized liquified gas due to depressurization can act like an explosion which could lead blast waves that usually called BLEVE (Boiling Liquid Expanding Vapor Explosions)

Task description:

- Literature review on phase transition in liquefied gasses during depressurization
- Continue working on model development for waves in compressible liquid and phasetransition rates
- Develop values needed for linear equations of state
- Compare modelling work with experimental data

Student category: EET and PT

Is the task suitable for online students (not present at the campus)? Yes

Practical arrangements:
The first developed model in implemented in Matlab and uses a two-phase solver. The fluids are modelled using linear EOSs.

Supervision:
As a general rule, the student is entitled to 15-20 hours of supervision. This includes necessary time for the supervisor to prepare for supervision meetings (reading material to be discussed, etc).

Signatures:

Supervisor (date and signature):

Appendix B: Thermodynamics Data Calculation of CO_2 during Depressurization in Matlab from Saturation State (293K) to 4Mpa.

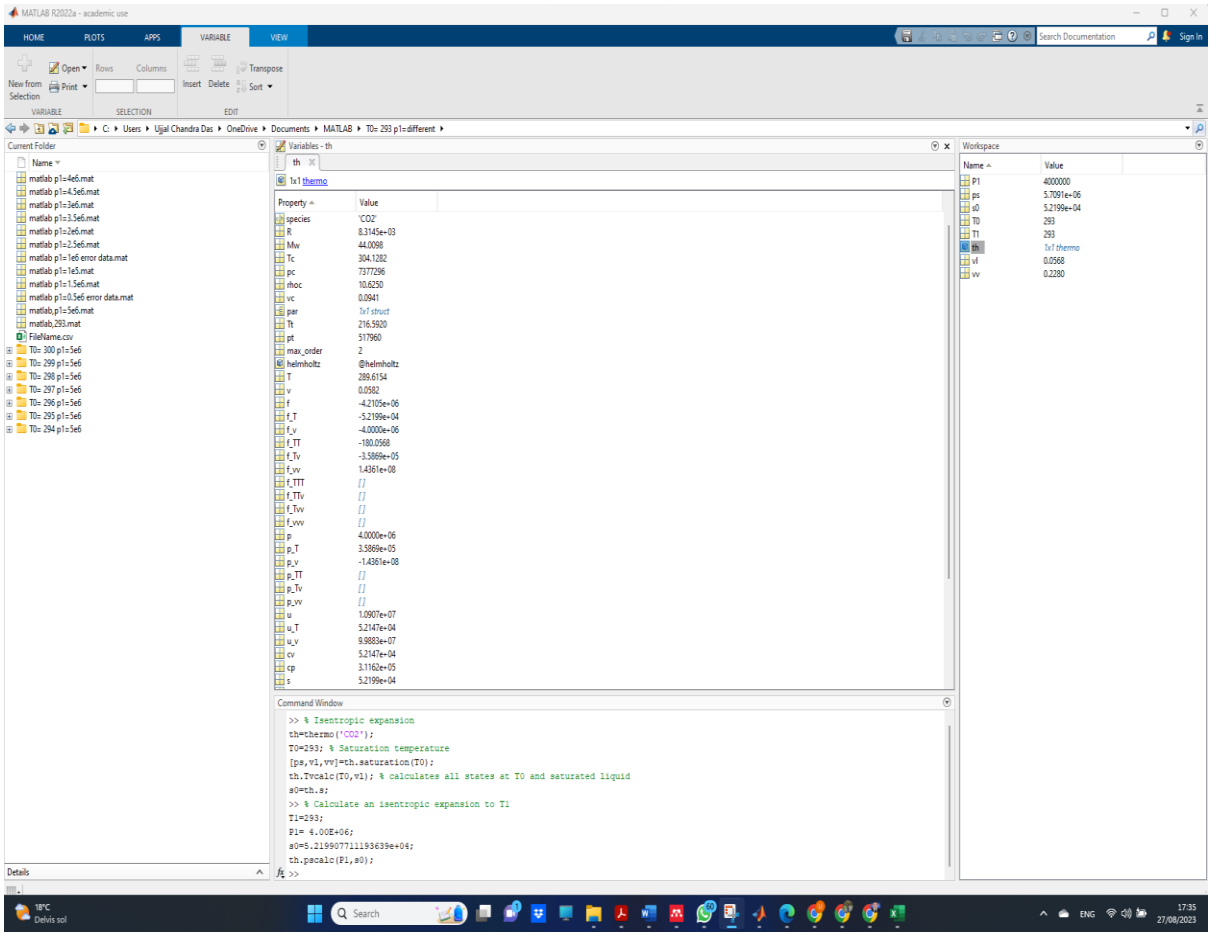

Figure 1: A Snapshot of Isentropic Expansion Data Calculation by Matlab.

Appendix C: Density Estimation of CO_2 at Temperature 293K Pressure 4Mpa.

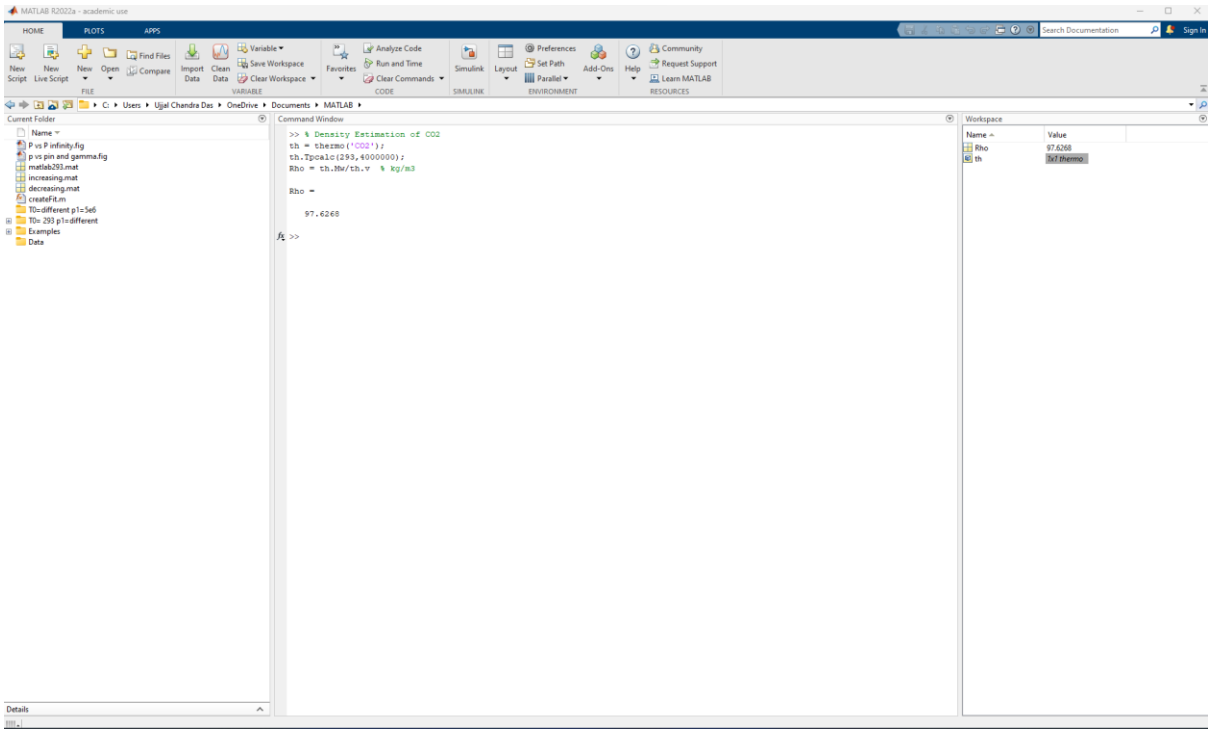

Figure 2: A Snapshot of Density Estimation of CO_2 by Matlab.